Effect of oxygen isotope substitution on magnetic ordering in $(La_{1-y}Pr_y)_{0.7}Ca_{0.3}MnO_3$

V. Pomjakushin

Laboratory for Neutron Scattering, ETH Zürich and PSI, Villigen

A. Balagurov

I.M. Frank Laboratory of Neutron Physics, JINR, Dubna

D. Sheptyakov

Laboratory for Neutron Scattering, ETH Zurich and PSI, Villigen

K. Conder, E. Pomjakushina

Laboratory for Developments and Methods, PSI

Laboratory for Neutron Scattering, ETH Zürich and PSI, Villigen

Large isotope effect in metallic manganites

Decrease in ($T_C \sim t^*$) by $^{16}O \rightarrow {}^{18}O$ exchange

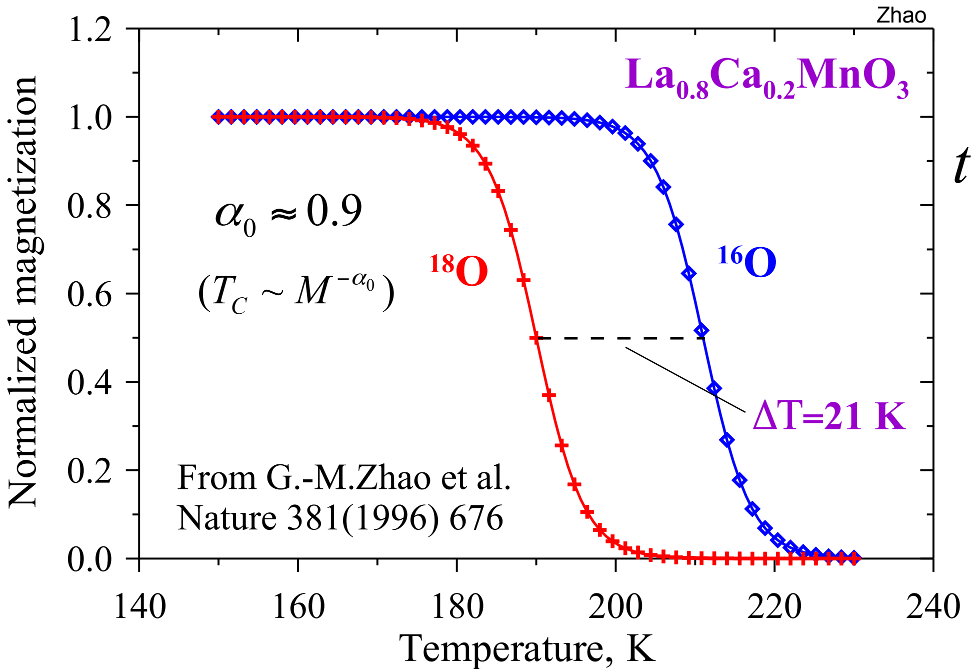

Oxygen isotope exponent $(T_C \sim M^{-\alpha_0})$

$$\alpha_0 = -\Delta \ln T_C / \Delta \ln M$$

Polaronic narrowing[1-3] of bandwidth t

$$t^* = t \exp(-g^2)$$

,where $g^2 = \lambda \cdot zt/\omega$ is coupl. const

$$\omega \sim M^{-0.5}$$

$$\alpha_0 = -\Delta \ln T_C / \Delta \ln M \sim 0.5 E / \hbar\omega$$

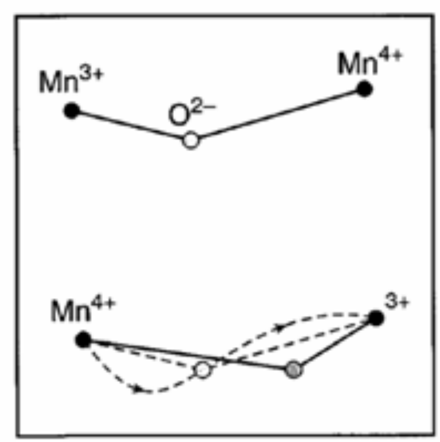

Schematic of possible dynamic distortion

$\alpha_0 \approx 0.8 - 1$ can be theoretically estimated[1]

1. L. P. Gor' kov and V. Z. Kresin, Phys. Rep. **400**, 149 (2004).
2. A.S.Alexandrov, N.F.Mott Int. J. Mod. Phys **8,** 2075 (1994)
3. A.S.Alexandrov, V.V.Kabanov, D.K.Ray, PRB **49,** 9915 (1994)

Isotope effect expected if:

Polaronic narrowing works:

e-hopping time $\tau \sim 1/\omega$ opt. phonon ~20 meV

Isotope effect expected?

YES

double-exchange
charge ordering
$T_C \sim zt^*$
$T_{CO} \sim t^*/V$, V~0.2

NO

Superexchange
$J_{AF} \sim -b^2/U$
$J_F \sim b^3/U^2$

$\tau = \hbar/U$, $U \sim 5$eV

<u>Isotope effect allows us to verify the type of interactions involved!</u>

Giant isotope effect in intermediate-bandwidth manganites

$^{16}O \longrightarrow {}^{18}O$

$T_C \longrightarrow 0$ K?

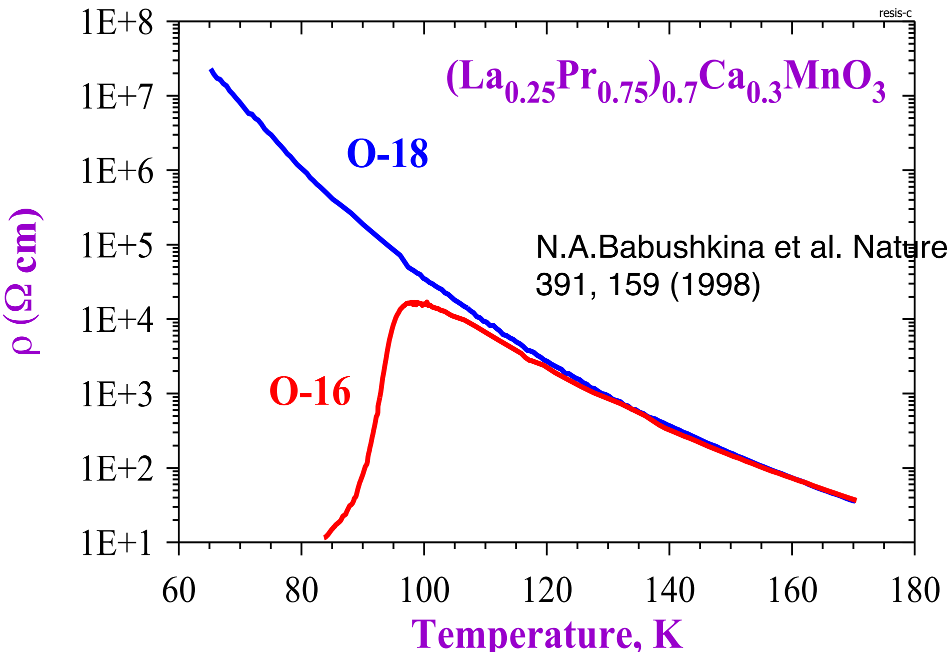

N.A.Babushkina et al. Nature 391, 159 (1998)

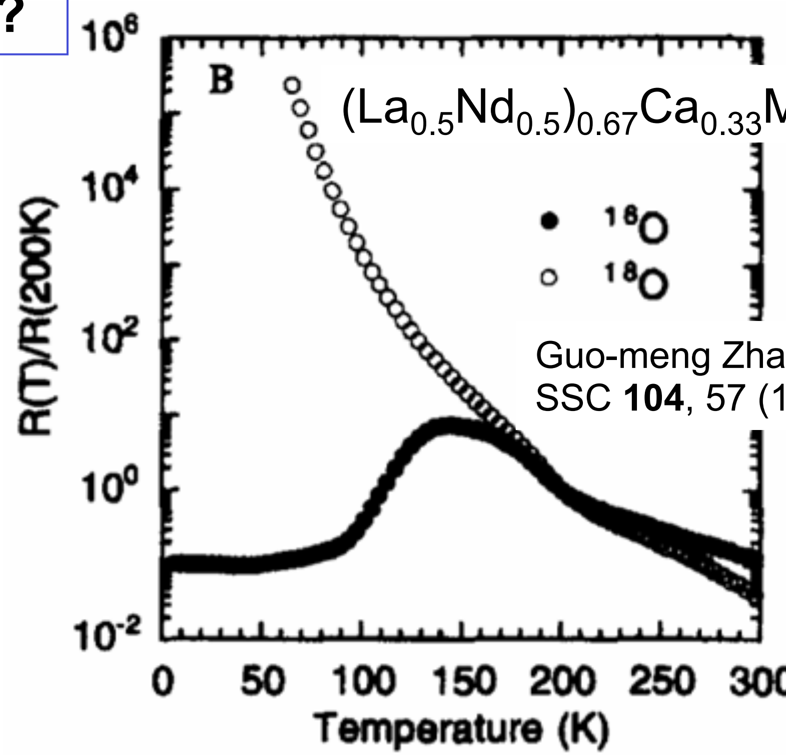

Guo-meng Zhao et al, SSC **104**, 57 (1997)

$$t^* = t\exp(-\frac{E_{pol}}{\varpi})$$ is not enough!

M-I is a percolate-type transition in phase separated state

Giant isotope effect in$(La_{1-y}Pr_y)_{0.7}Ca_{0.3}MnO_3$, y=0.75

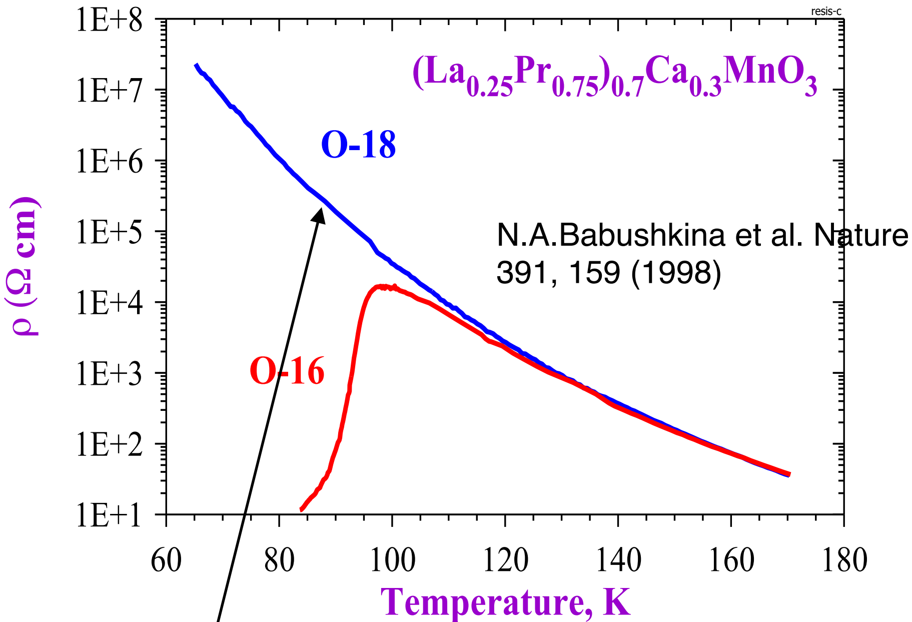

Neutron diffraction intensities

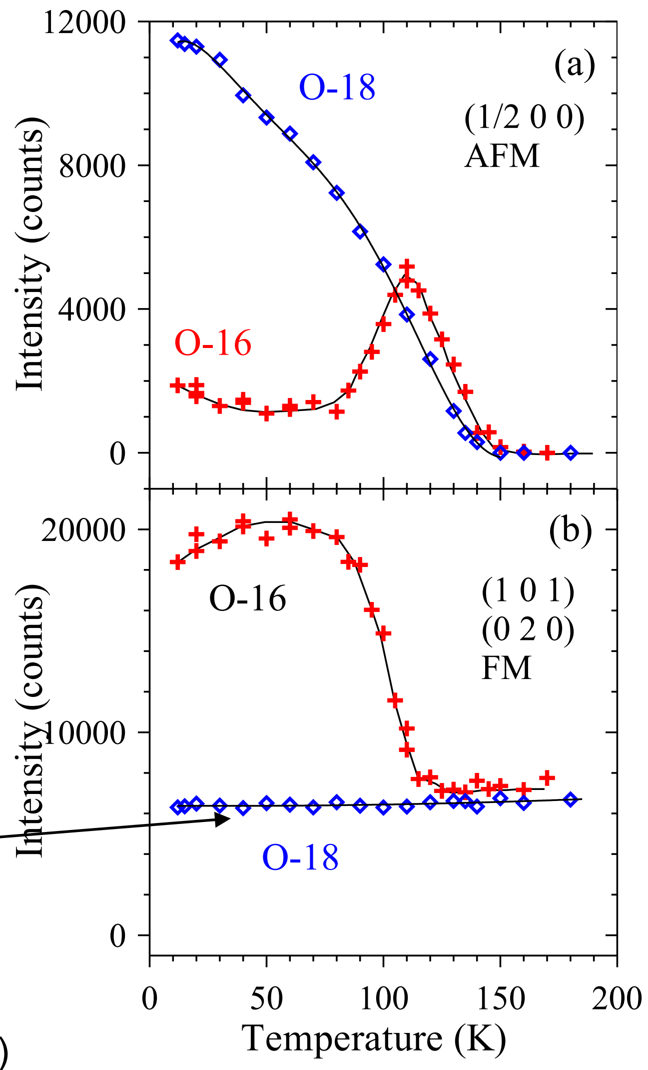

Increase in the m_O leads to complete suppression of the FMM phase and hence to the insulating state

Balagurov et al, *Phys. Rev. B* **60**, 383 (1999); *B* **64**, 24420, (2001)

$(La_{1-y}Pr_y)_{0.7}Ca_{0.3}MnO_3$ phase diagram

A-cation

Mott insulattor ← FM double exchange metal

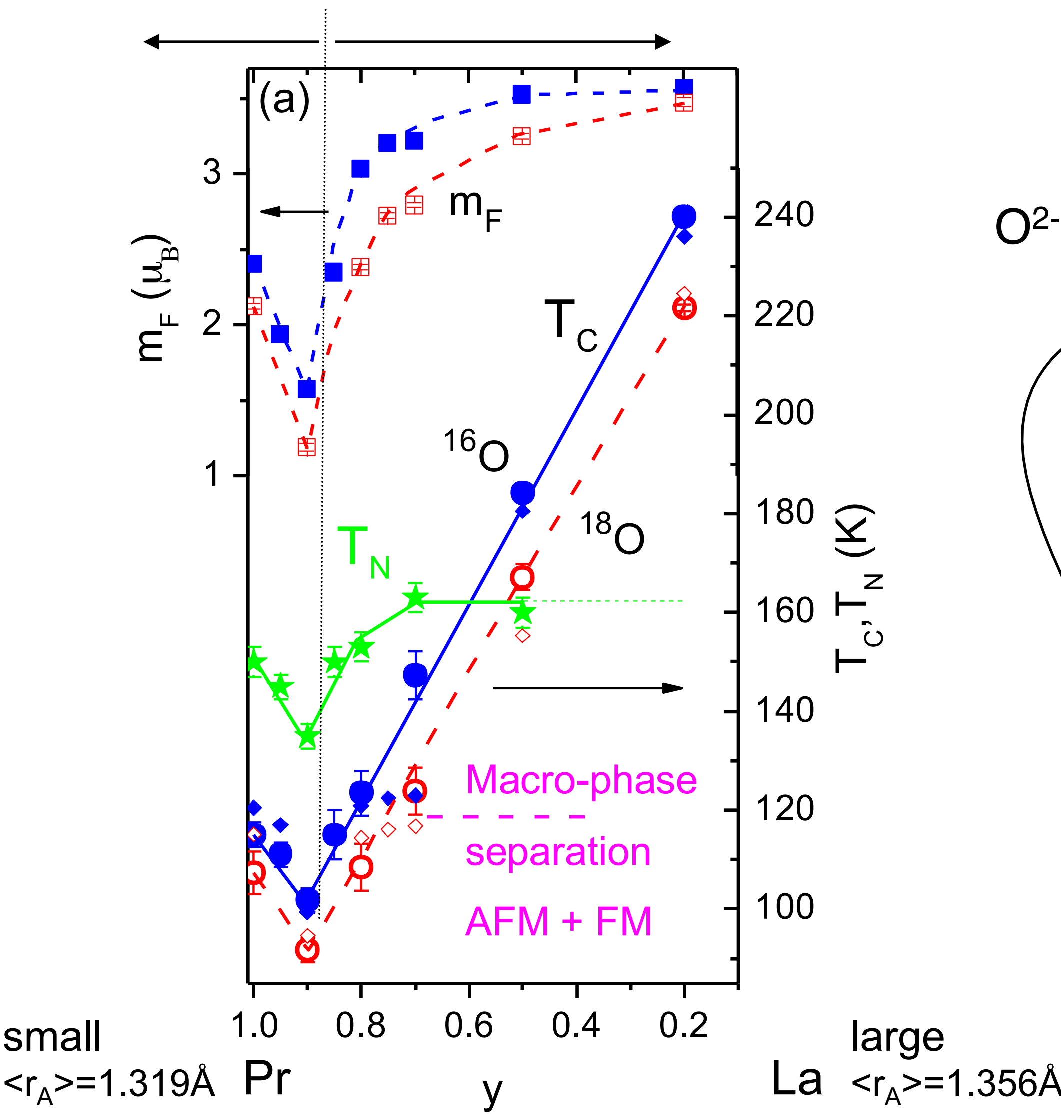

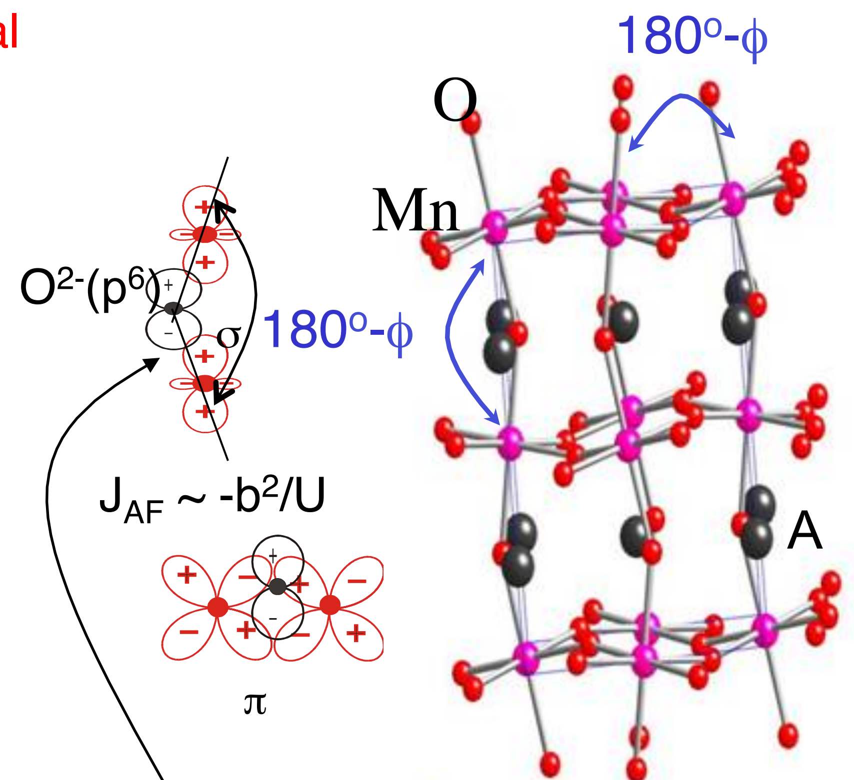

(Mn-O) electron transfer integral

$b_\sigma \sim \cos(\phi) \sim <r_A> \sim (1-y)$

is increased with *y* resulting in the insulator-metal transition

$(La_{1-y}Pr_y)_{0.7}Ca_{0.3}MnO_3$ phase diagram

Mott insulattor ← FM double exchange metal

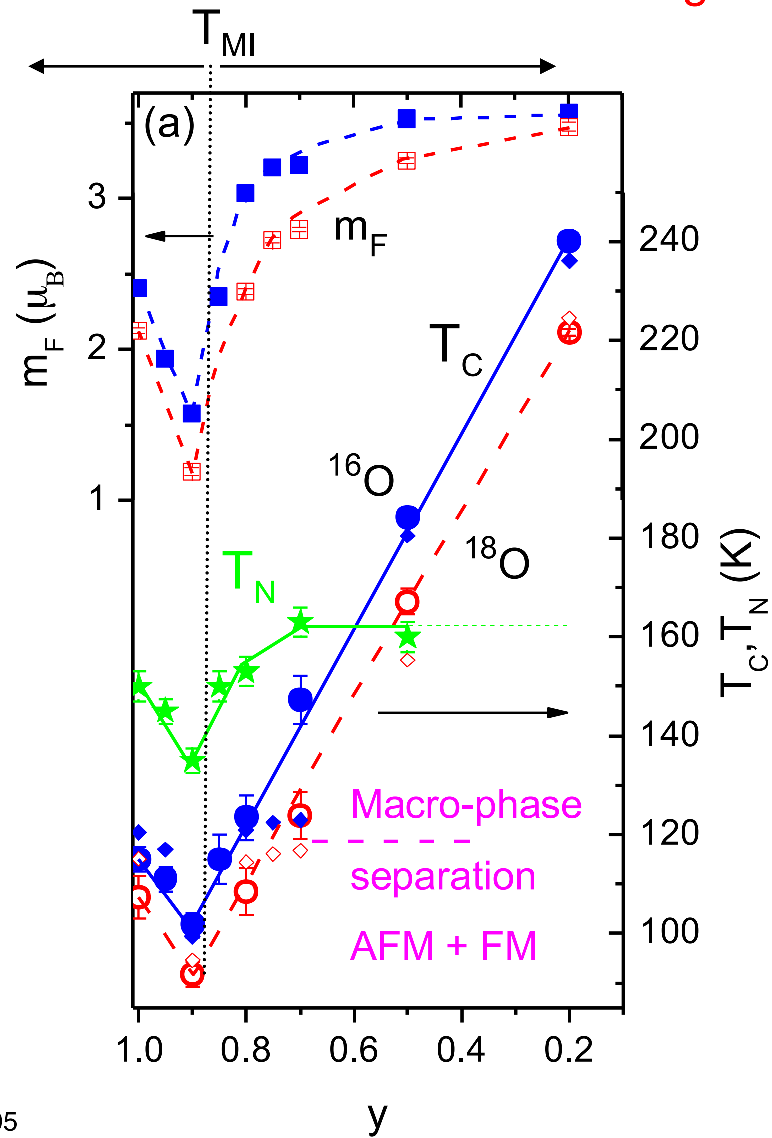

Mn-O-Mn valence bond angles

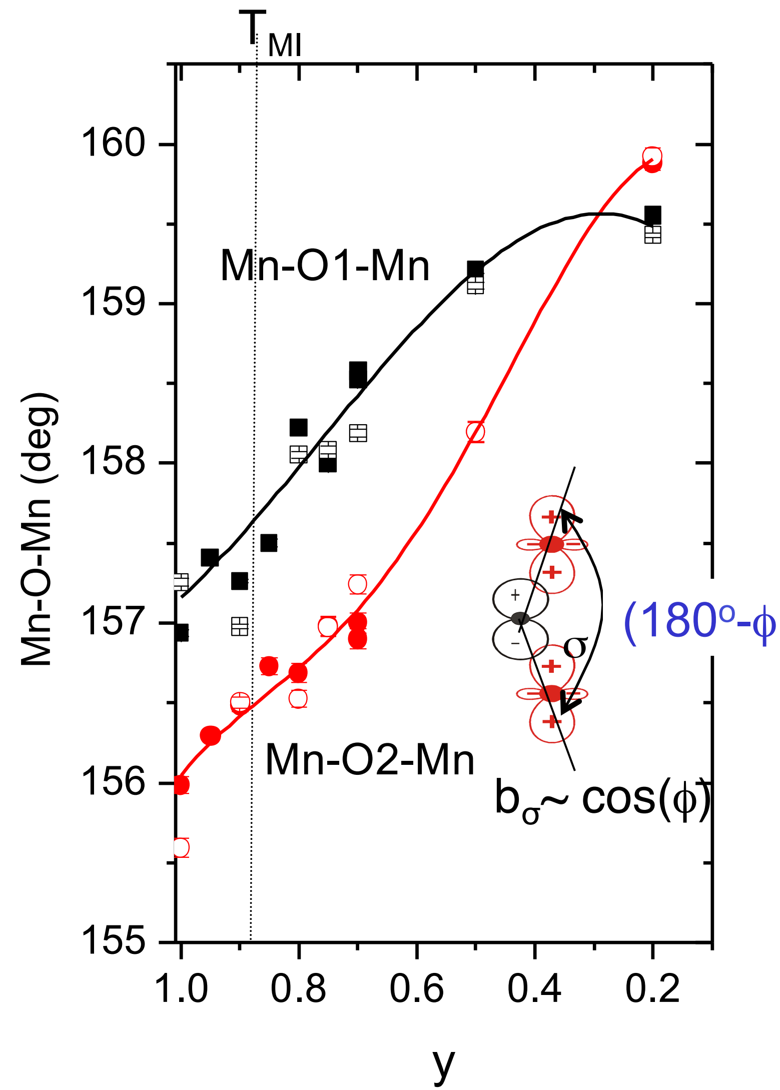

$(La_{1-y}Pr_y)_{0.7}Ca_{0.3}MnO_3$ phase diagram

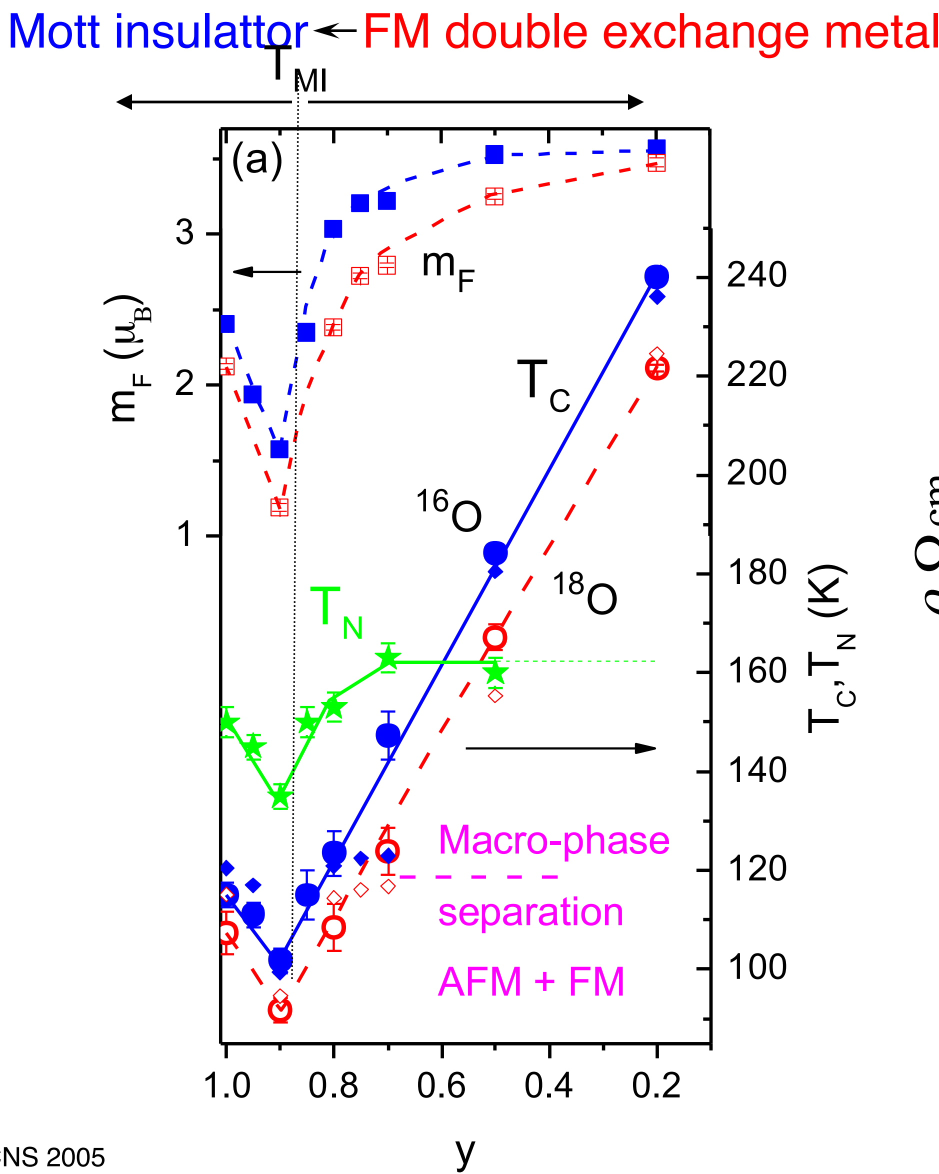

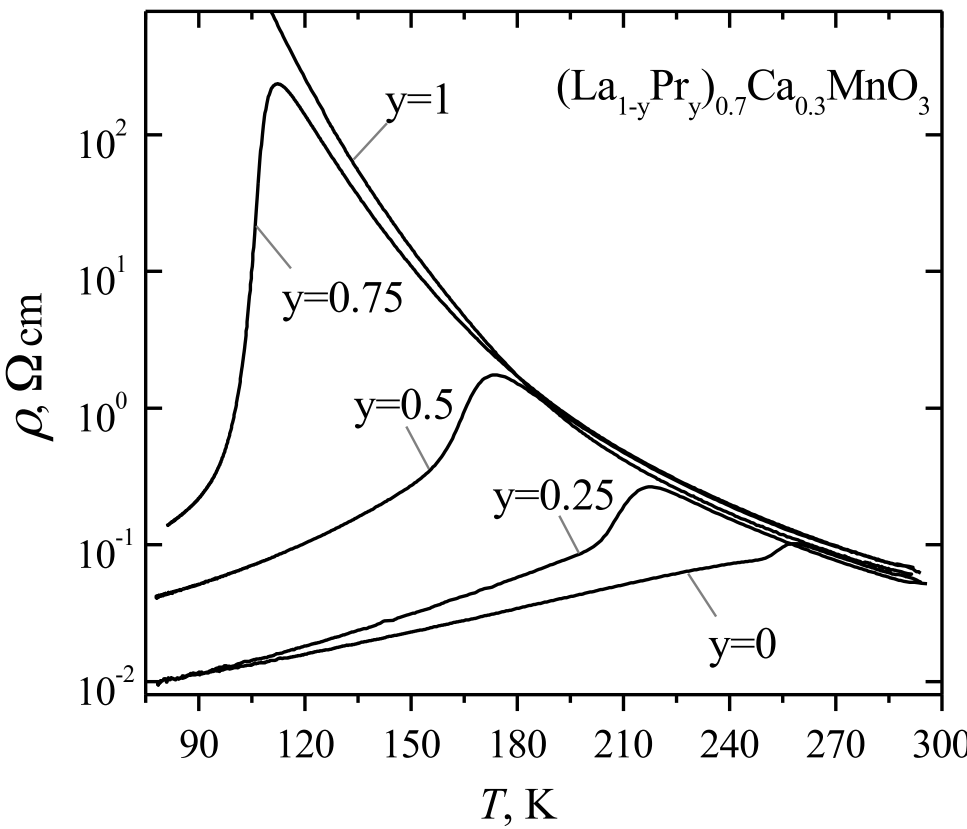

Samples

Powders of $(La_{1-y}Pr_y)_{0.7}Ca_{0.3}MnO_3$

- **O-series (y=0.2, 0.5, 0.7, 0.75, 0.8, 0.85, 0.9, 0.95 1.0):** by the solid state synthesis from oxides and carbonates of respective metals. The ^{18}O (>85%) samples as well as the final ^{16}O samples were obtained via respective oxygen isotope exchange at the same conditions

- **N-series**[1]: by the "paper" synthesis starting from aqueous solutions of nitrates of the respective metals (N-series) with the final thermal treatment similar to the O-series

[1] Balagurov et al, *Phys. Rev. B* **60**, 383 (1999);
Phys. Rev. B **64**, 024420-1 (2001);
Eur. Phys. J. B **19**, 215 (2001)

Experiment

1. Neutron (T=2-1400K) and synchrotron x-ray (room T) diffraction

High resolution HRPT diffractometer,
Cold DMC (up to 4.2Å) at SINQ/PSI

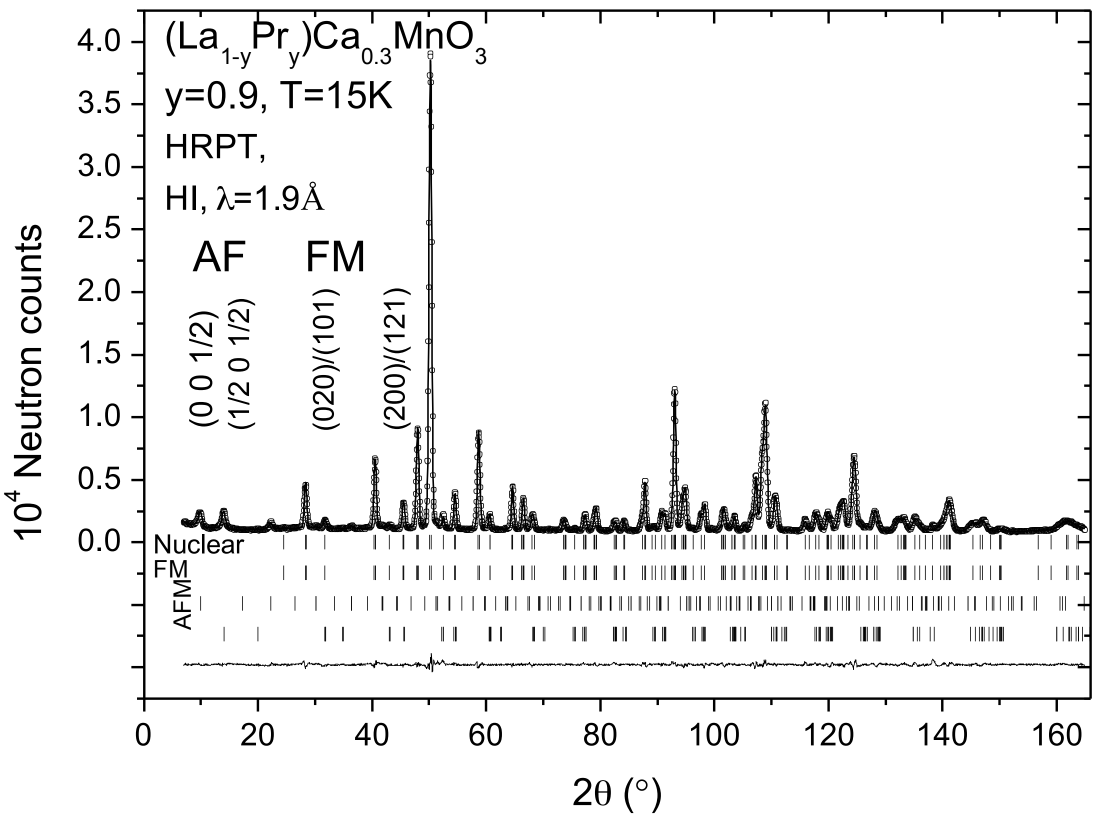

MS beamline at SLS/PSI

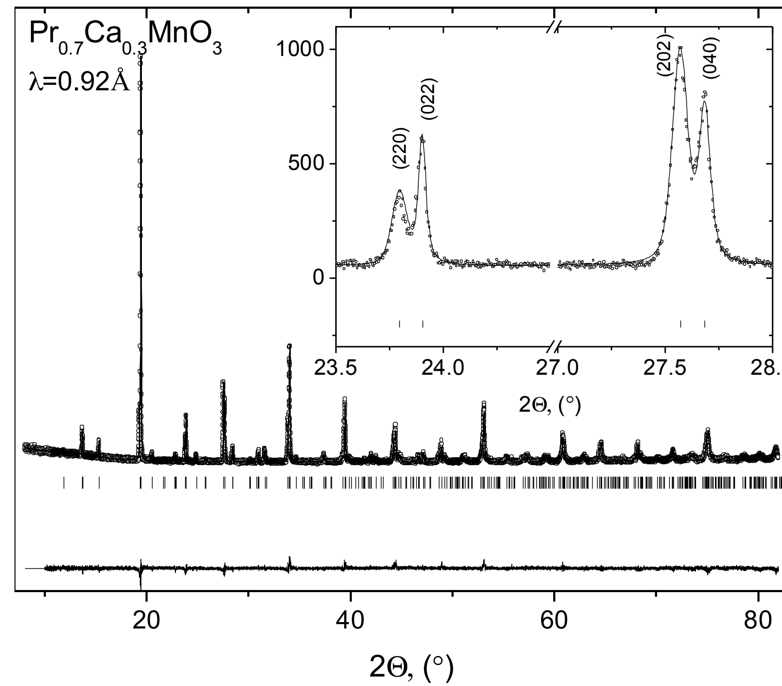

2. ac-magnetic susceptibility, T=2K-400K

Magnetic structure as a function of temperature

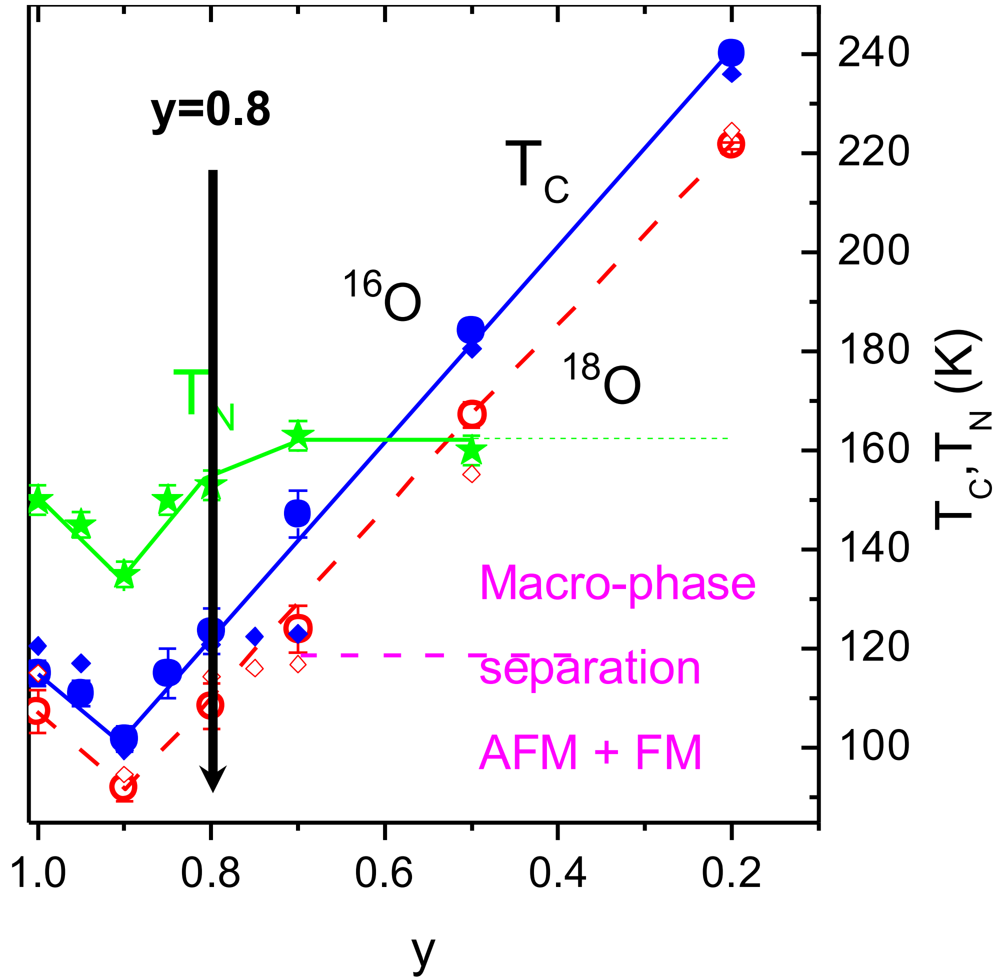

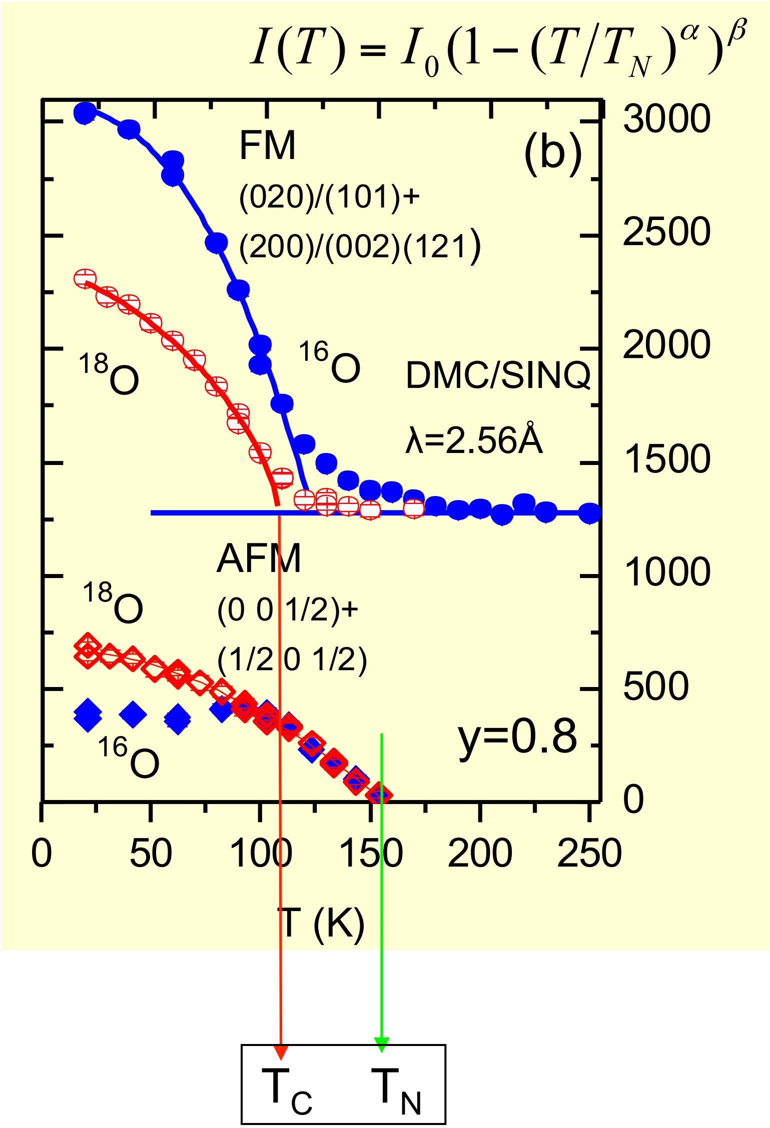

Magnetic structure as a function of temperature

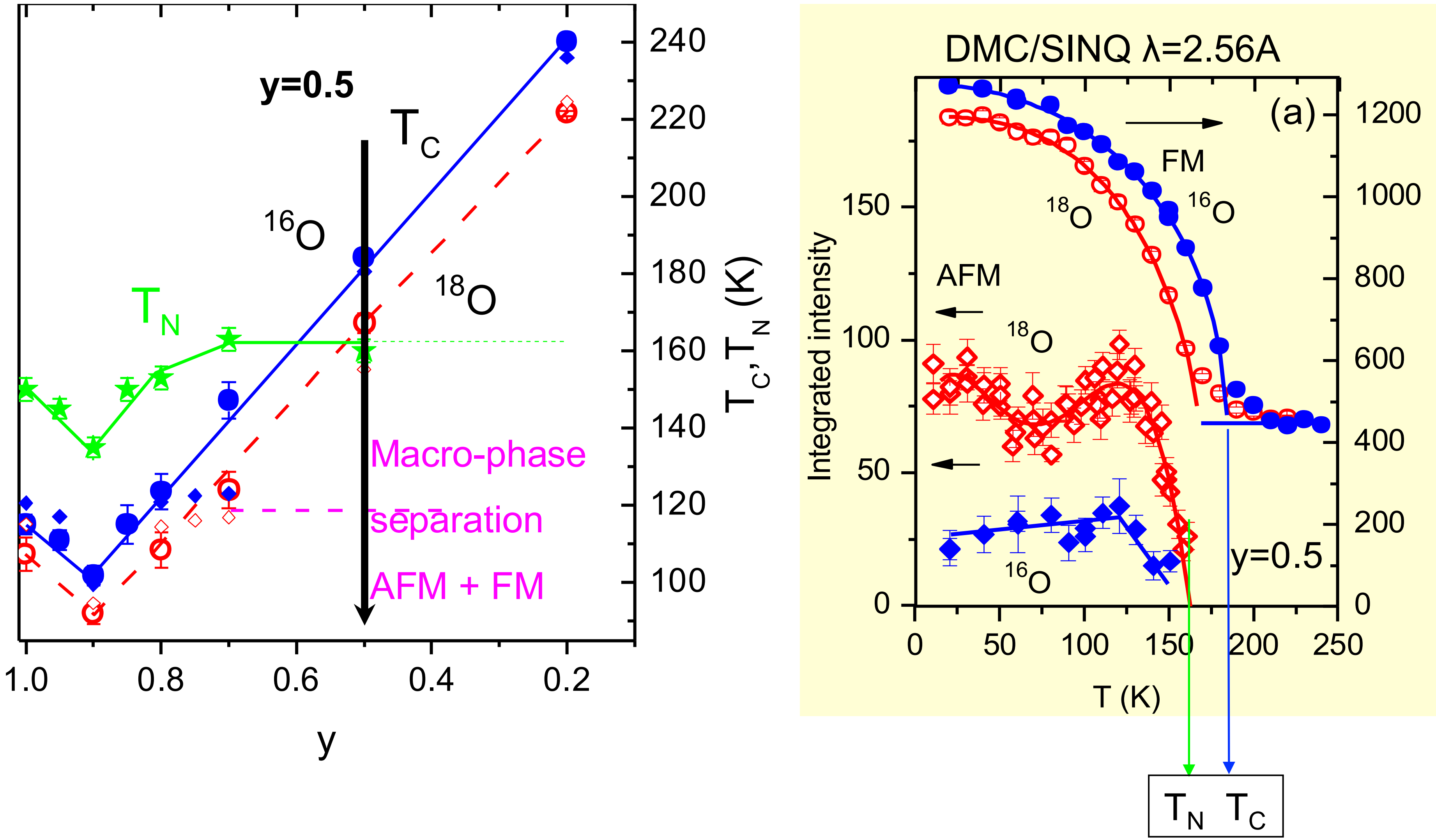

Ground magnetic state of $(La_{1-y}Pr_y)_{0.7}Ca_{0.3}MnO_3$

Effective moments

$$m_F^2(m_A^2) = M_F^2\left(1 - \frac{m_A^2}{M_A^2}\right)$$

$M_A = 2.26(1)\mu_B$
$M_F = 3.57(2)\mu_B$

$m_A = (1-\nu)^{1/2} M_A$
$m_F = \nu^{1/2} M_F$

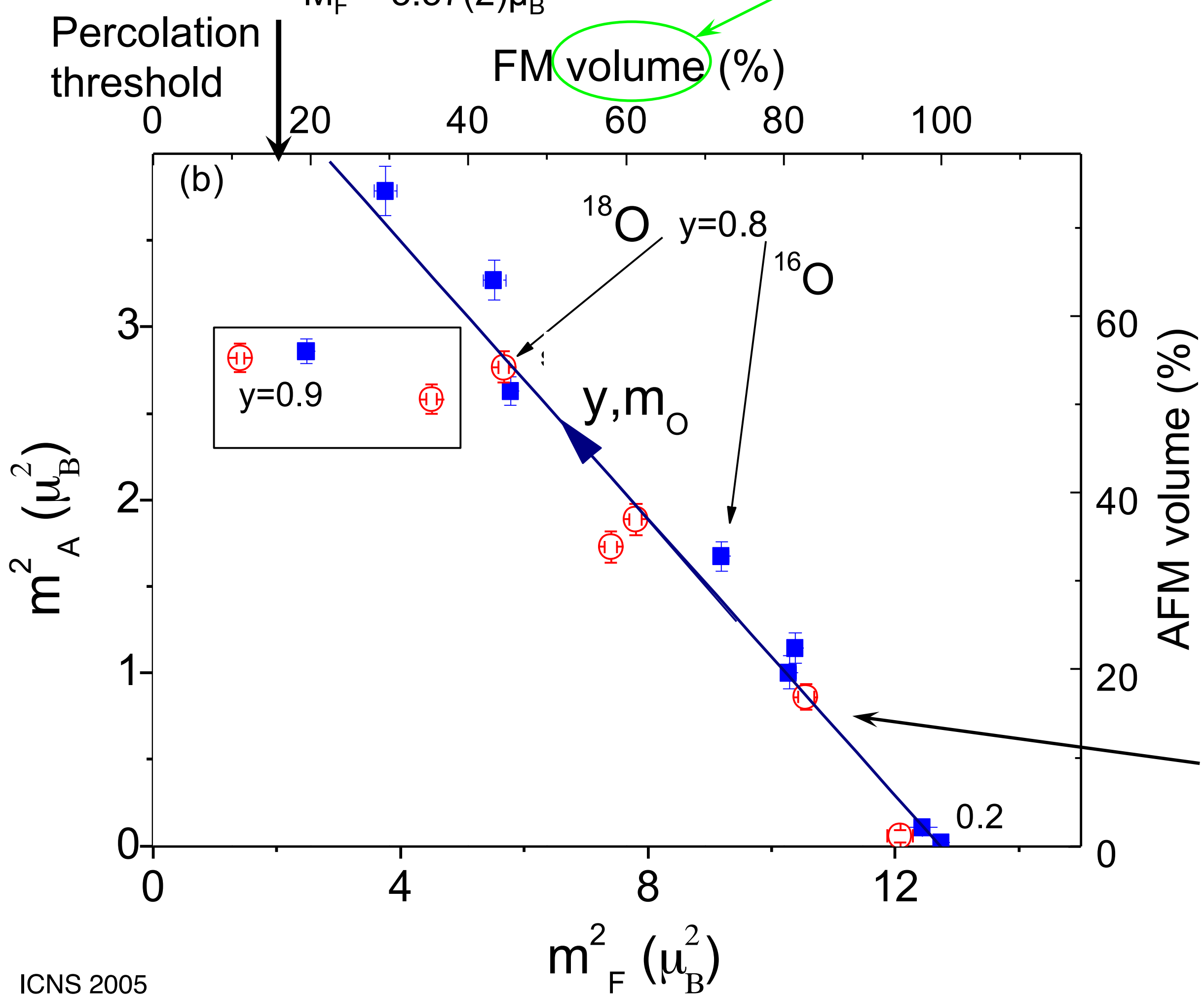

Effective FM moment as a function of Pr-conc.

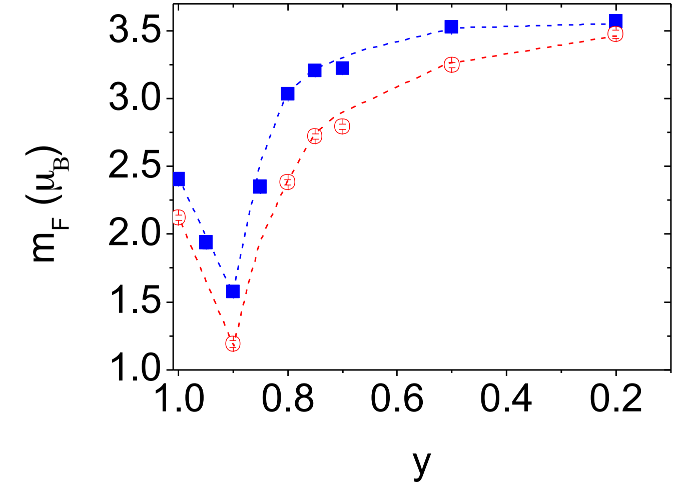

Polaronic narrowing acts as the narrowing due to the increase in *y:*

the phase balance is shifted towards the AFM/CO phase.

Microstrains effect on phase separation in $(La_{1-y}Pr_y)_{0.7}Ca_{0.3}MnO_3$

Phase separation is favored by internal micro-strains!

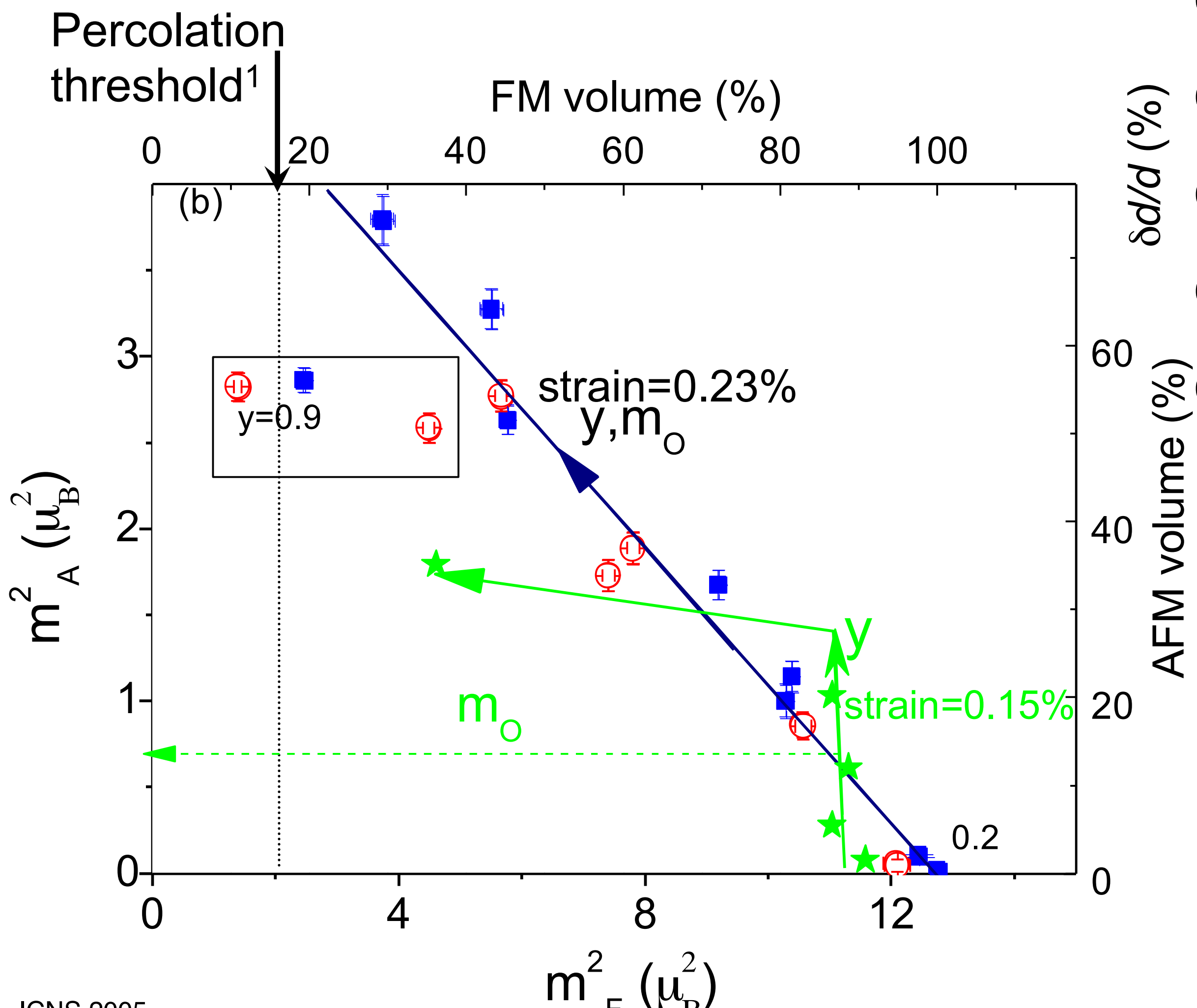

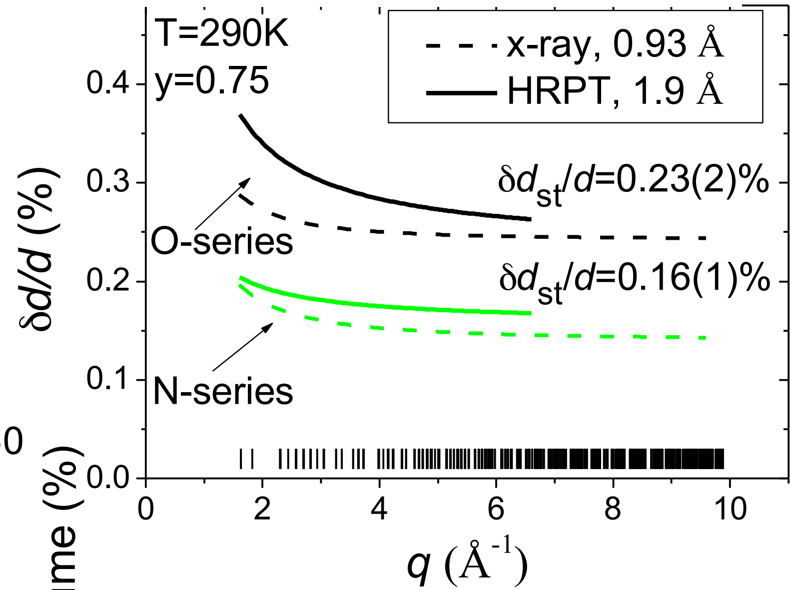

Suppression of all types of ordering near M-I transition in $(La_{1-y}Pr_y)_{0.7}Ca_{0.3}MnO_3$

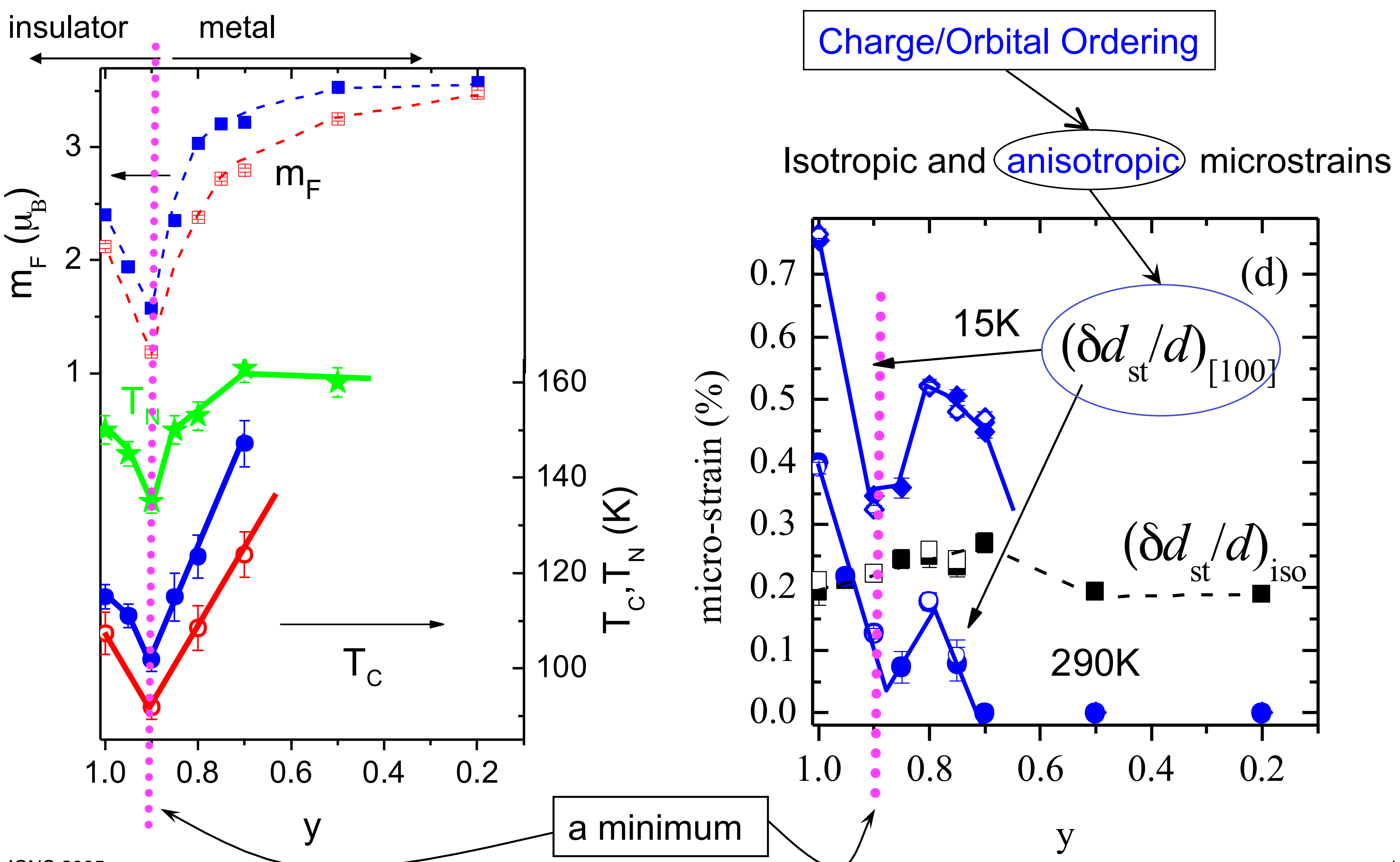

Influence of quenched disorder on the competition between ordered states separated by a first-order transition

J.Burgy, A.Moreo, M. Mayr, E.Dagotto, et al, PRL, PRB 2000-2004

$(La_{1-y}Pr_y)_{0.7}Ca_{0.3}MnO_3$

RFIM +correlated disorder

$$H = -J\sum_{\langle ij\rangle} s_i s_j + J'\sum_{[ik]} s_i s_k$$

$J' \rightarrow J'_{ik} = J' + W_{ik}$

α~3 elasticity mechanism of the distortion propagation (Khomskii, Kugel, 2001) ~ $1/d_{[ik]}^{\alpha}$

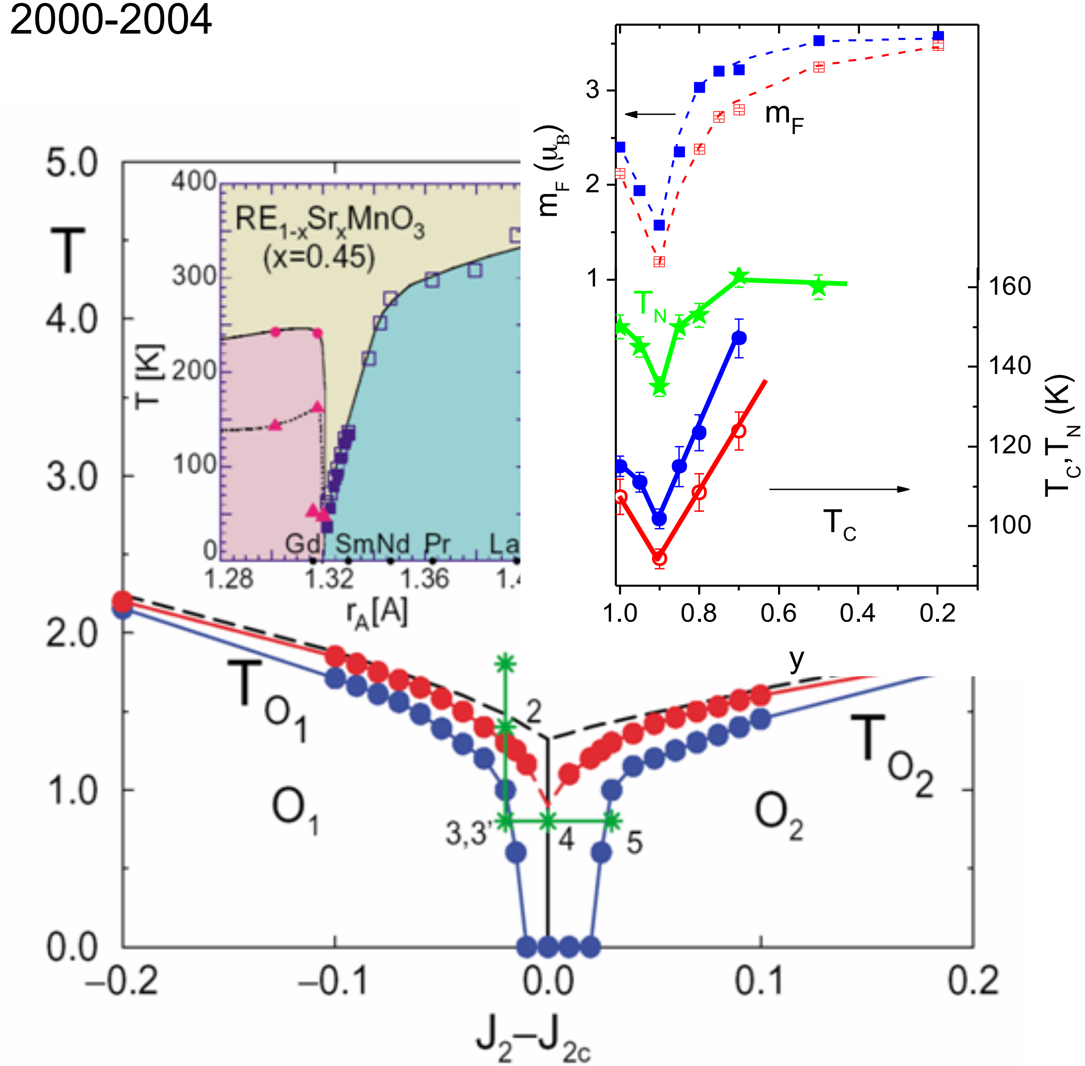

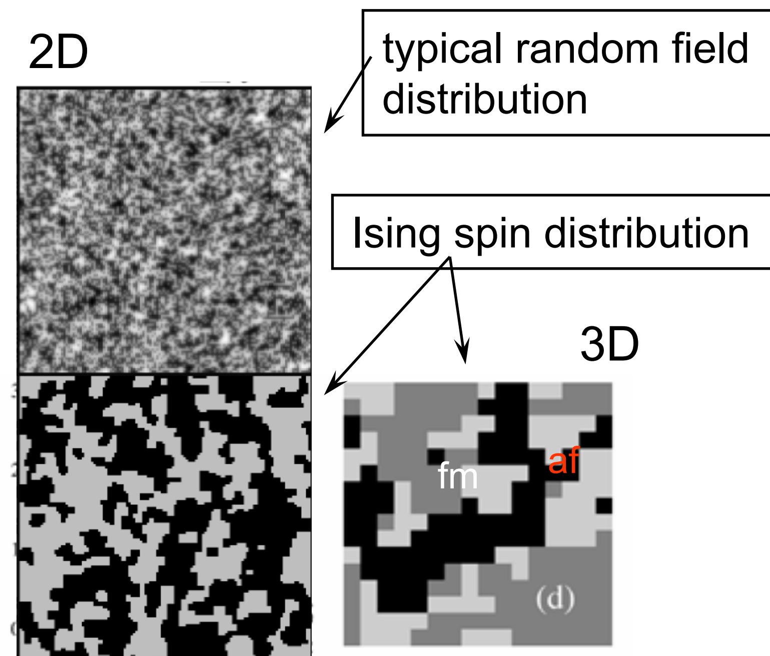

Summary

$(La_{1-y}Pr_y)_{0.7}Ca_{0.3}MnO_3$ (y=0.2-1.0) with ^{16}O/ ^{18}O

- polaronic narrowing of the carrier bandwidth and the crystal lattice micro-strains control the volume fractions of the mesoscopic FM and AFM clusters.
- phase separation is favored by the presence of the micro-strains.
- a quenched disorder is responsible for the formation of the long-scale phase separated state
- There exists a genuine FMI phase for $Pr_{0.7}Ca_{0.3}MnO_3$, but with the DE-kind of interactions involved.

The End

Pseudocubic-orthorhombic transition

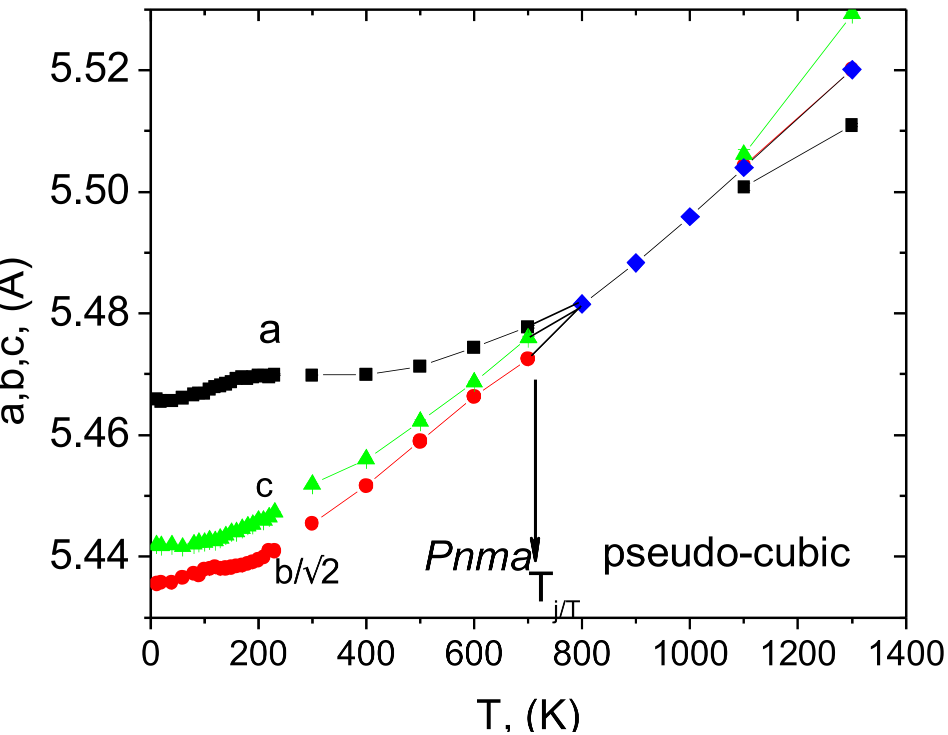

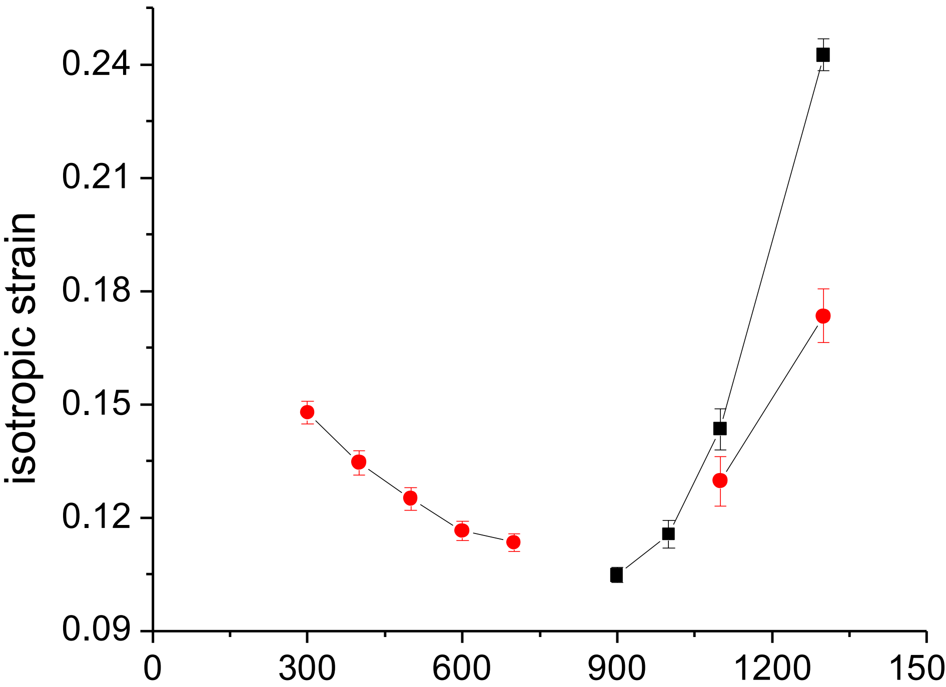

Microstructure parameters

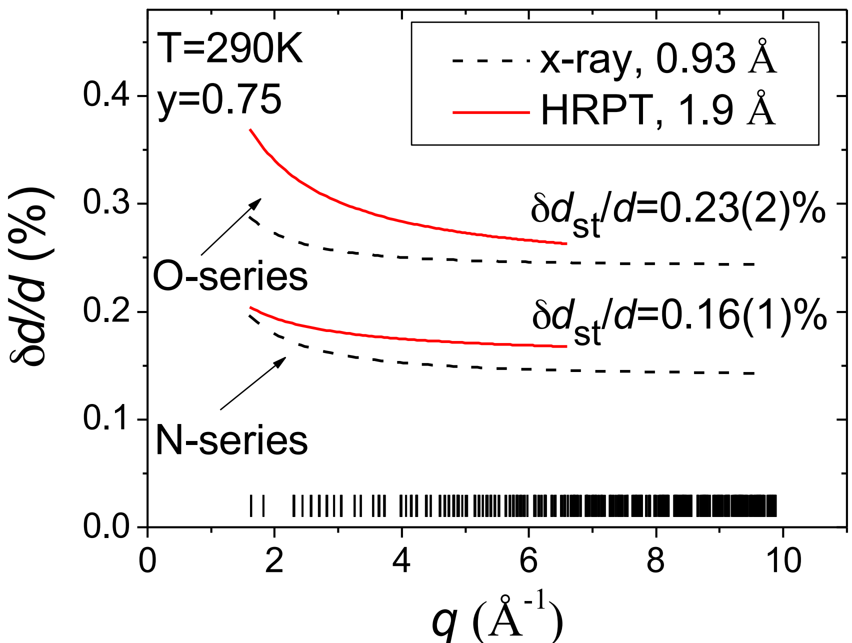

Bragg peak width

$\delta d/d = \delta a/a \otimes d/L \otimes$ "instrument"

strain size

Deconvolution of the pseudo-Voigt Bragg peaks width δ(2θ)="*Cagliotti*" with the instrument resolution function.

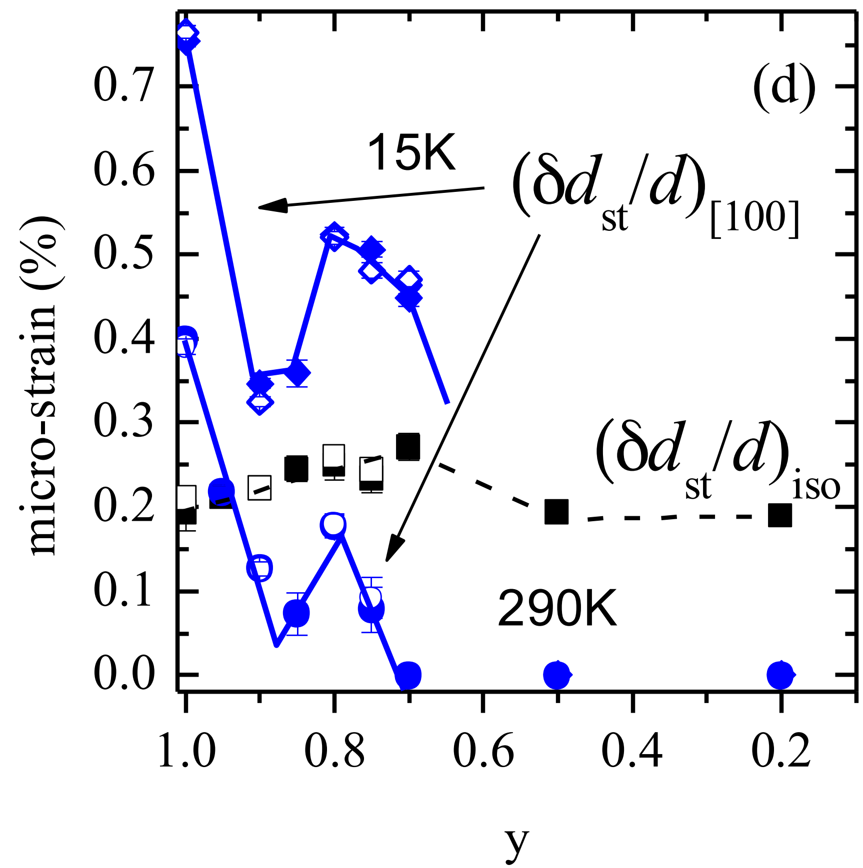

micro-strains as a function of Pr concentration (sp. gr. *Pnma*)

Orbital and Charge ordering

$(La_{1-y}Pr_y)_{0.7}Ca_{0.3}(Mn^{3+})_{0.7}(Mn^{4+})_{0.3}O_3$

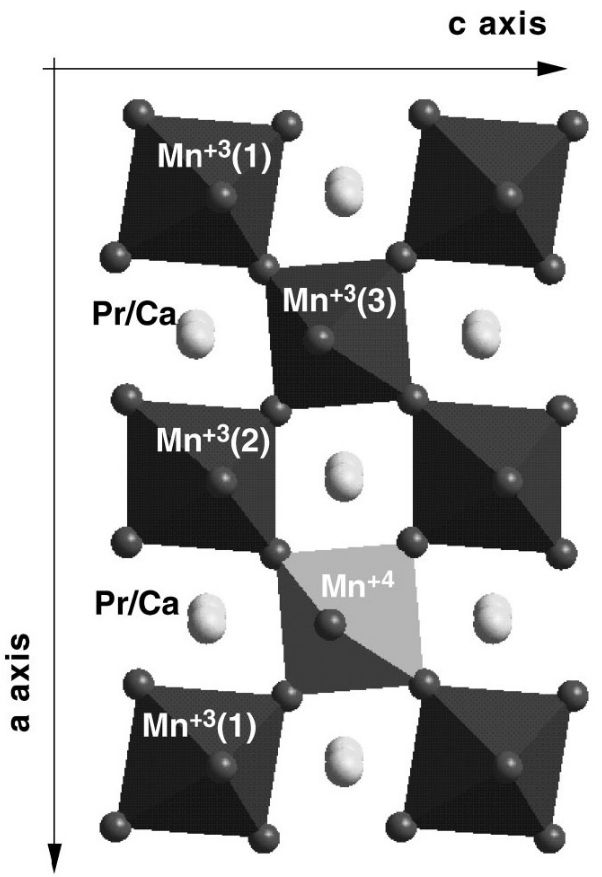

From D.E. Cox et al.,PRB (1998)

- satellite (to *Pnma*) Bragg peaks due to a-axis doubling
- anisotropic (along [100]) peak broadening due to the microstrains

Readily observed from NPD data

OO effects

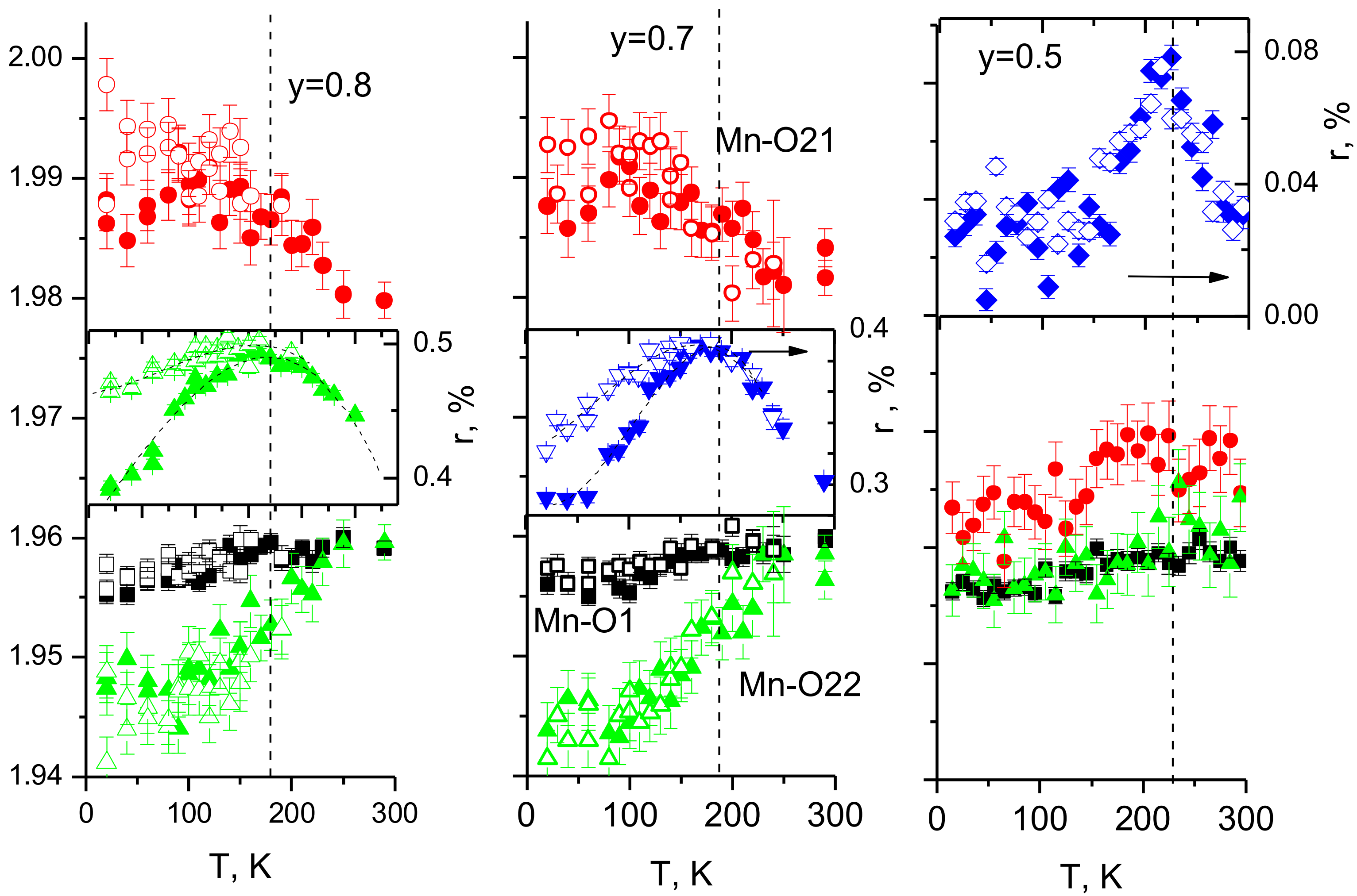

y=0.8
y=0.7
y=0.5
Mn-O21
Mn-O1
Mn-O22
r, %
T, K
2.00
1.99
1.98
1.97
1.96
1.95
1.94
0.5
0.4
0.3
0.08
0.04
0.00
0
100
200
300

$(La_{1-y}Pr_y)_{0.7}Ca_{0.3}MnO_3$: $\chi_{ac}(T)=\chi'(T)+i\chi''(T)$

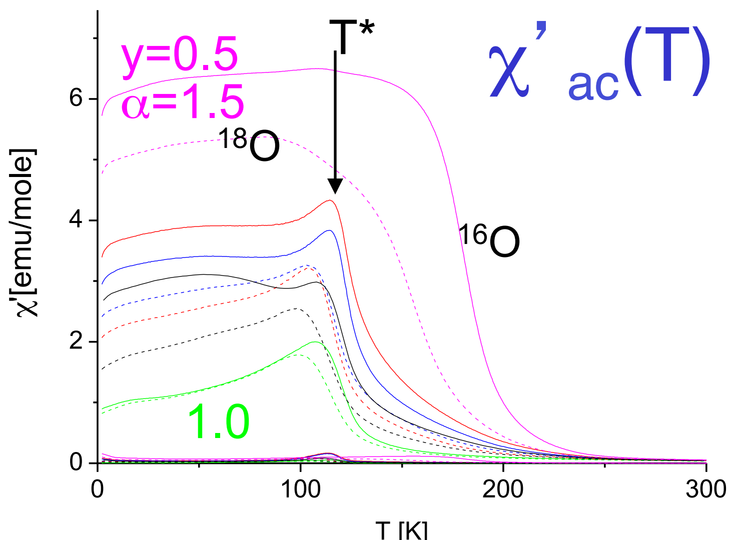

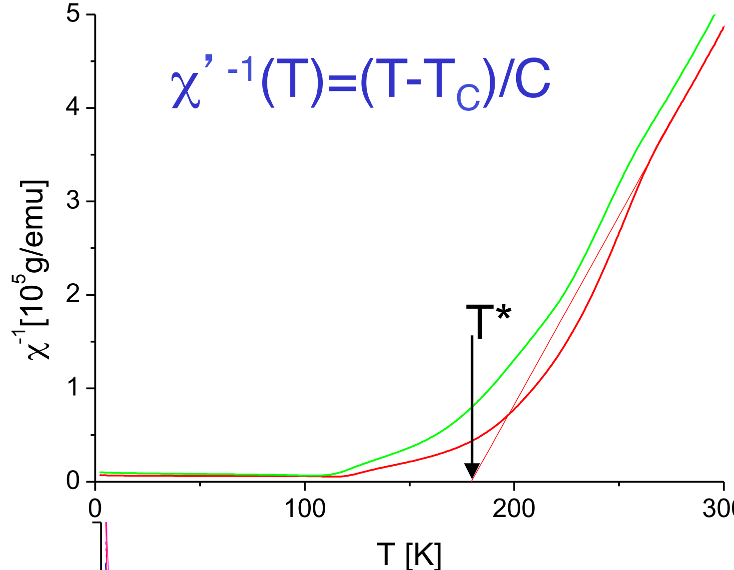

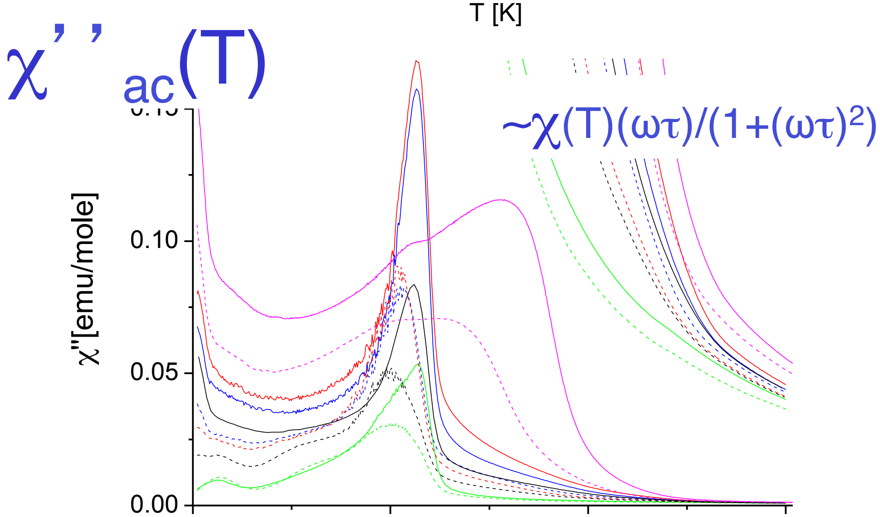

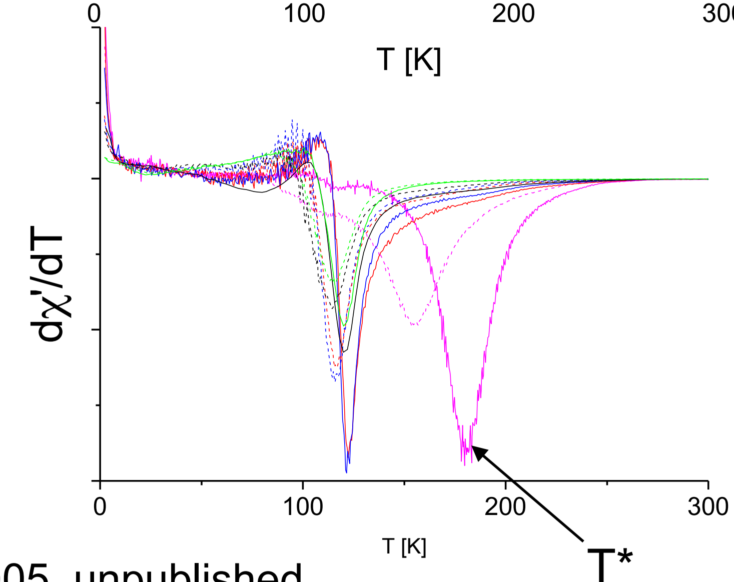

Pomjakushin et al, 2005, unpublished

Deconvolution of the Bragg-peak widths

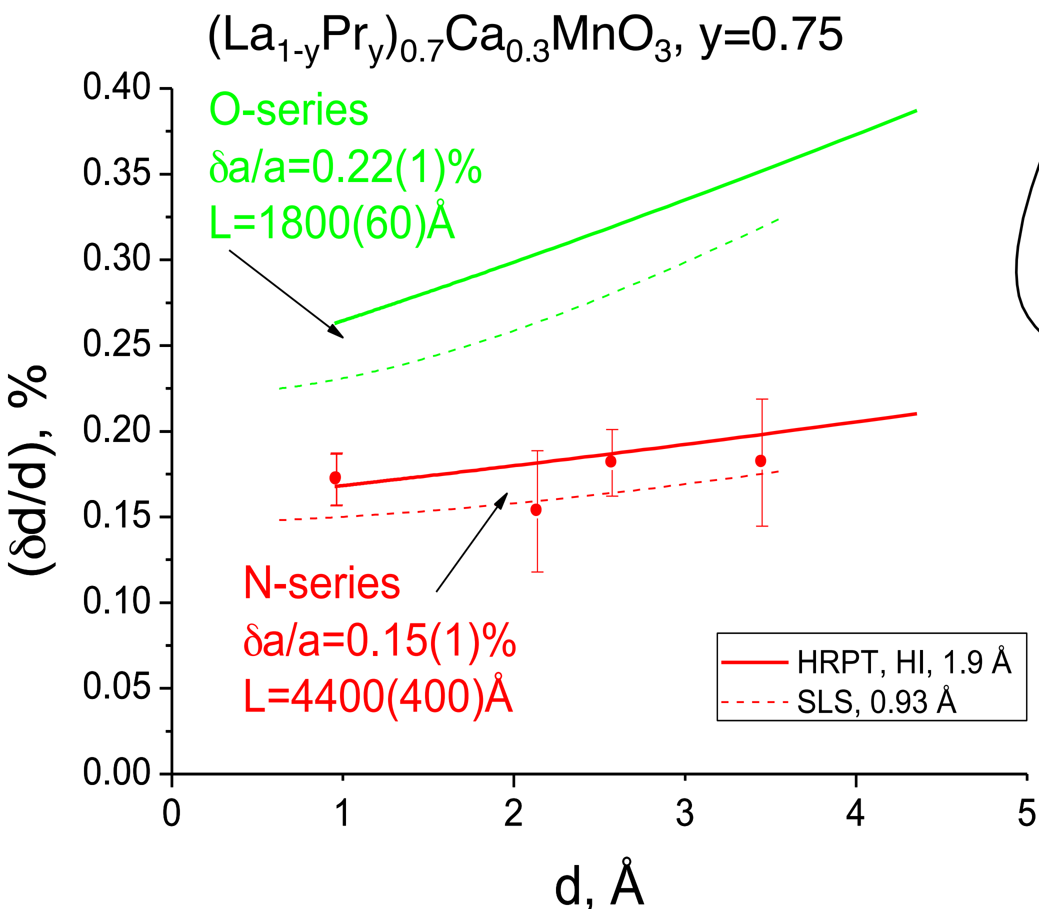

$$I_{\exp} = \int_{-\infty}^{\infty} PV_{sample}(2\theta - \xi) PV_{instrument}(\xi) d\xi$$

Deconvolution of the pseudo-Voigt Bragg peaks width δ(2θ)="*Cagliotti*" with the instrument resolution function.

<u>Bragg peak width</u>

δd/d= δa/a ⊗ d/L

strain size

PV=Pseudo-Voigt

Gaussian ⊗ Lorenzian

$$\int_{-\infty}^{\infty} G(2\theta - \xi) L(\xi) d\xi$$

T-dep of anisotropic strain

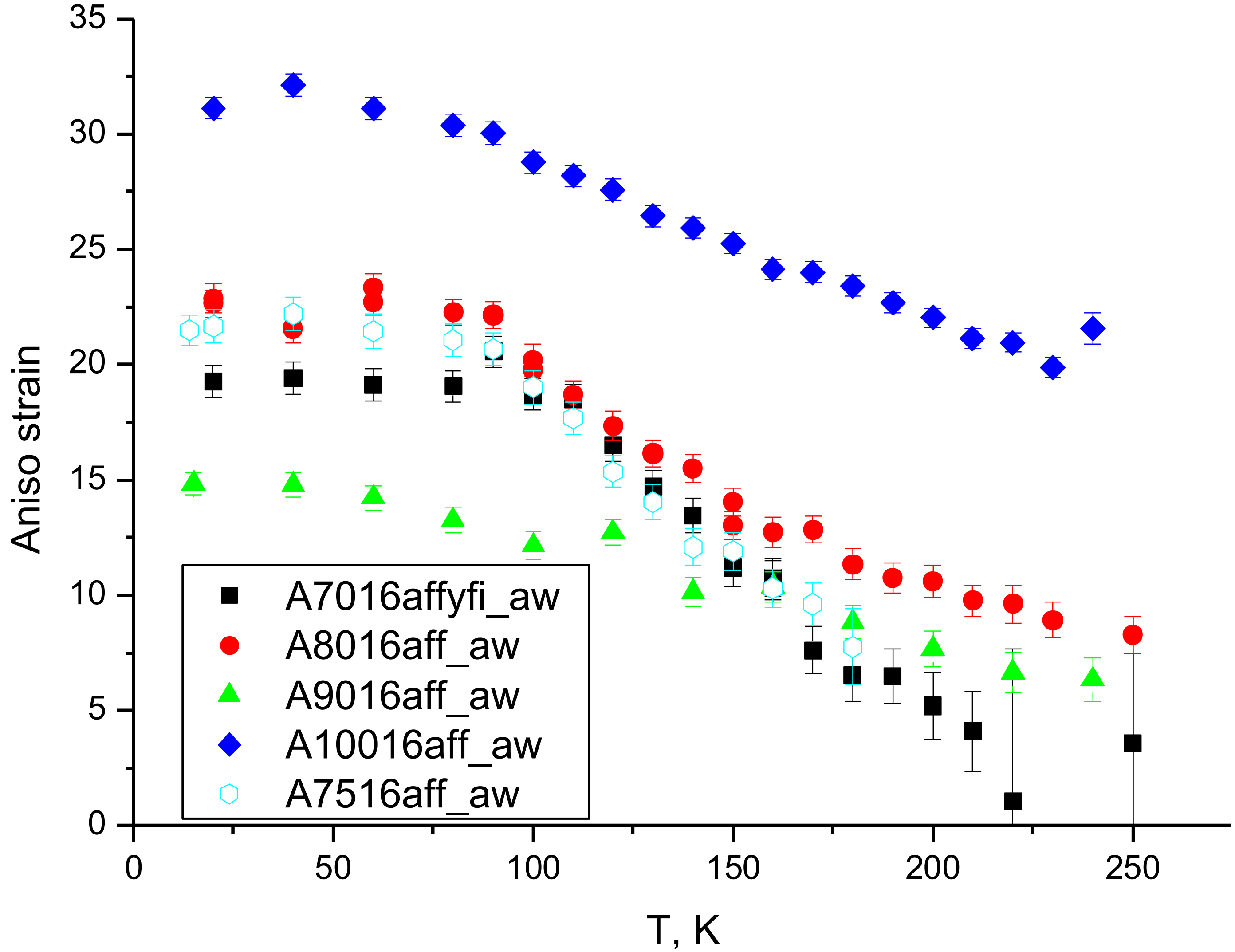

Thermal displacement parameters

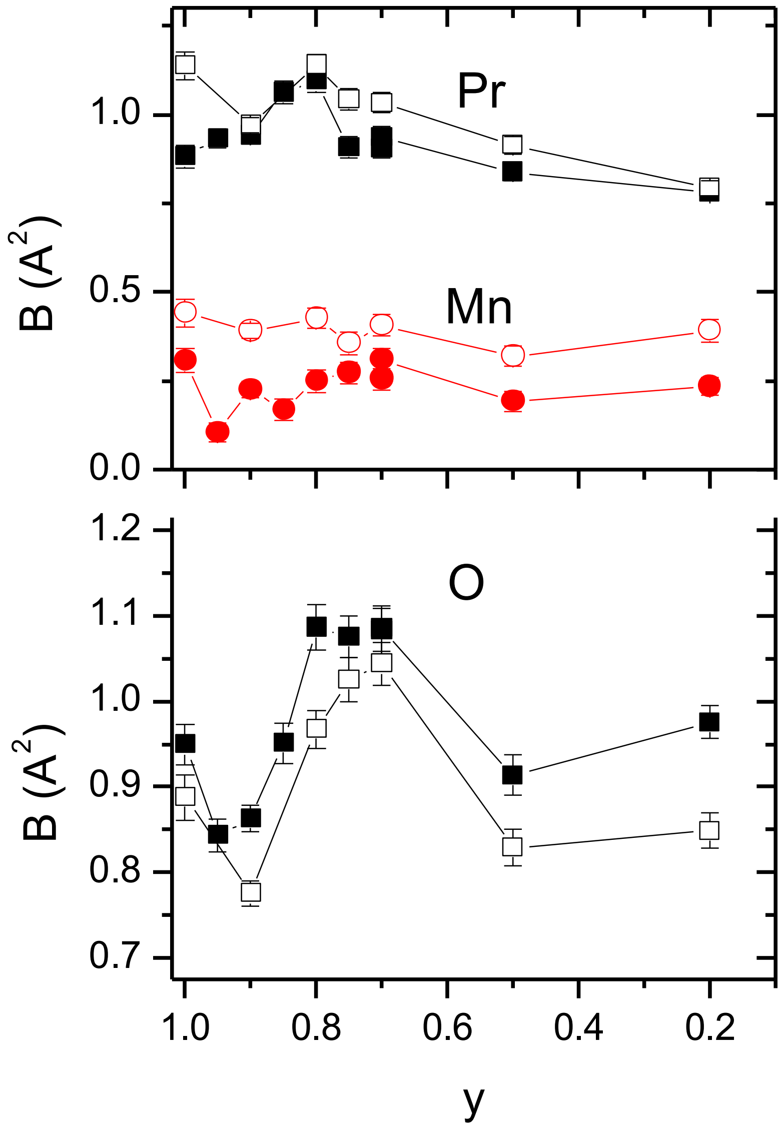

$B^{1/2} \sim T <1/\omega^2> 1/M$

a,b,c

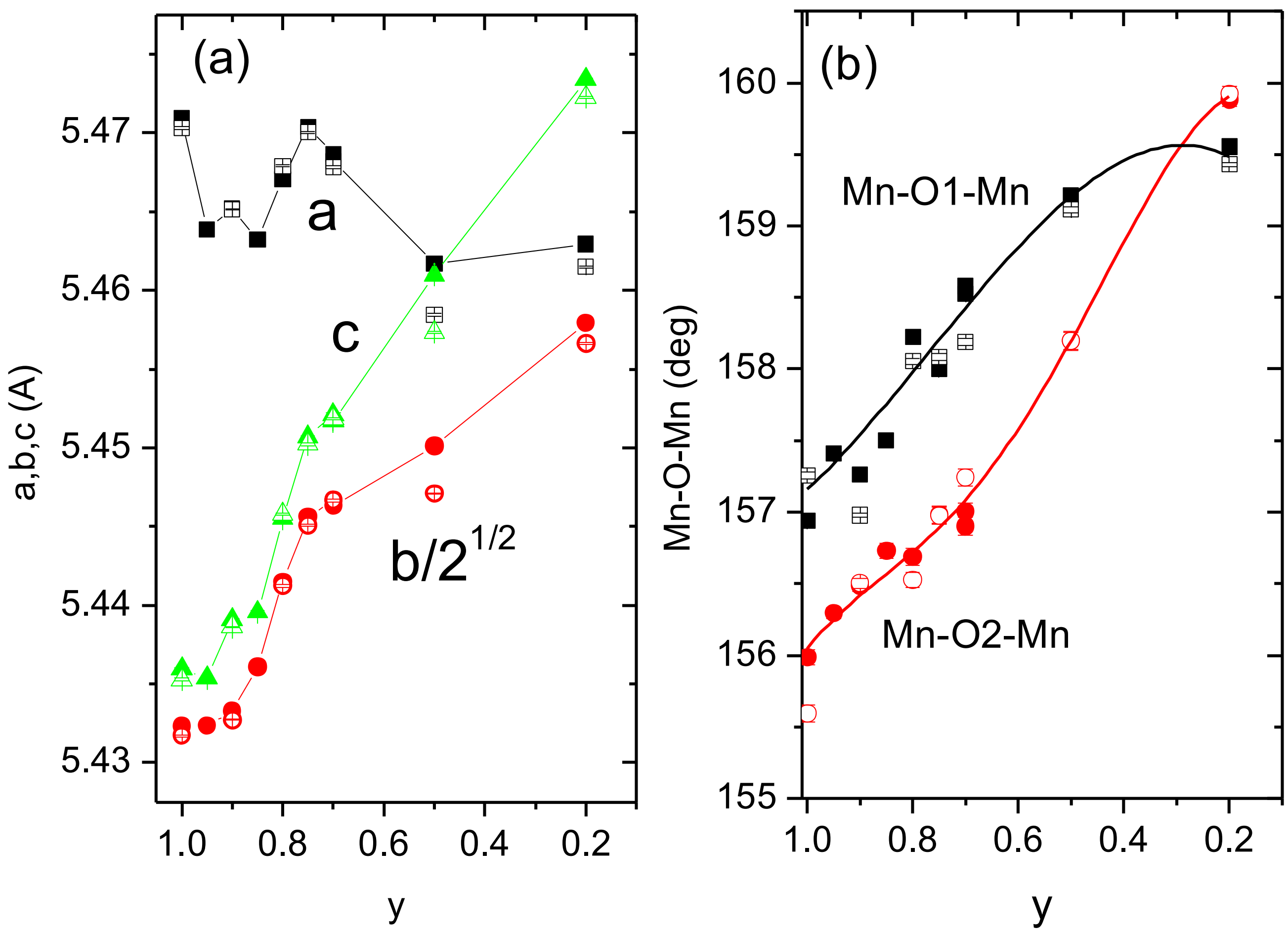

(a)
a
c
b/2^{1/2}
a,b,c (A)
5.47
5.46
5.45
5.44
5.43
1.0
0.8
0.6
0.4
0.2
y
(b)
Mn-O1-Mn
Mn-O2-Mn
Mn-O-Mn (deg)
160
159
158
157
156
155
1.0
0.8
0.6
0.4
0.2
y

Magnetic state. Bragg I(T)

x=0.8, 0.75. “New” O-series

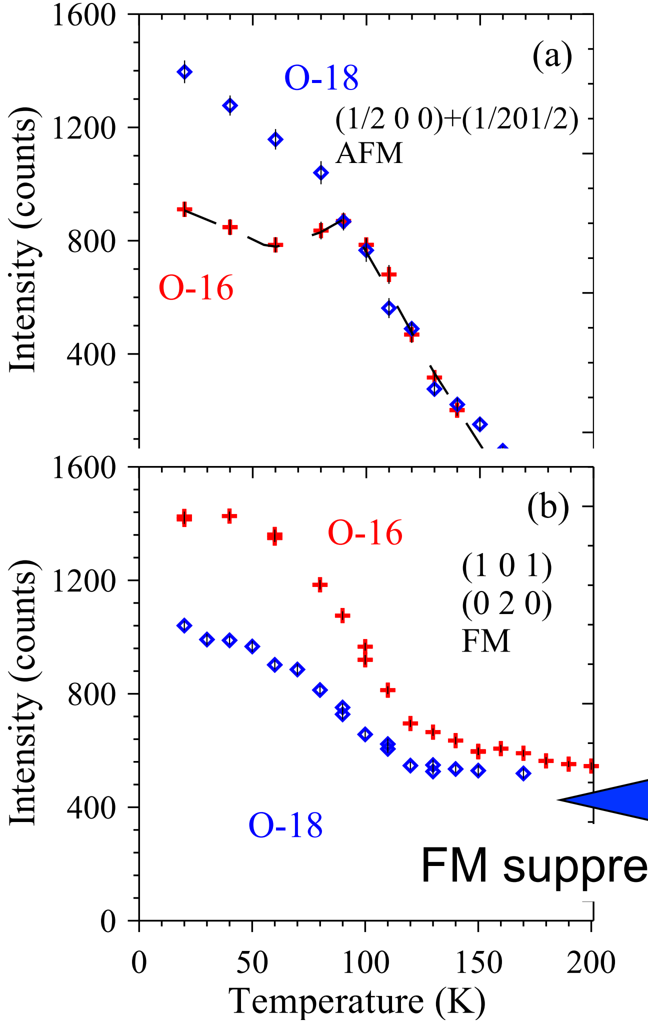

x=0.75. “Old” N-series

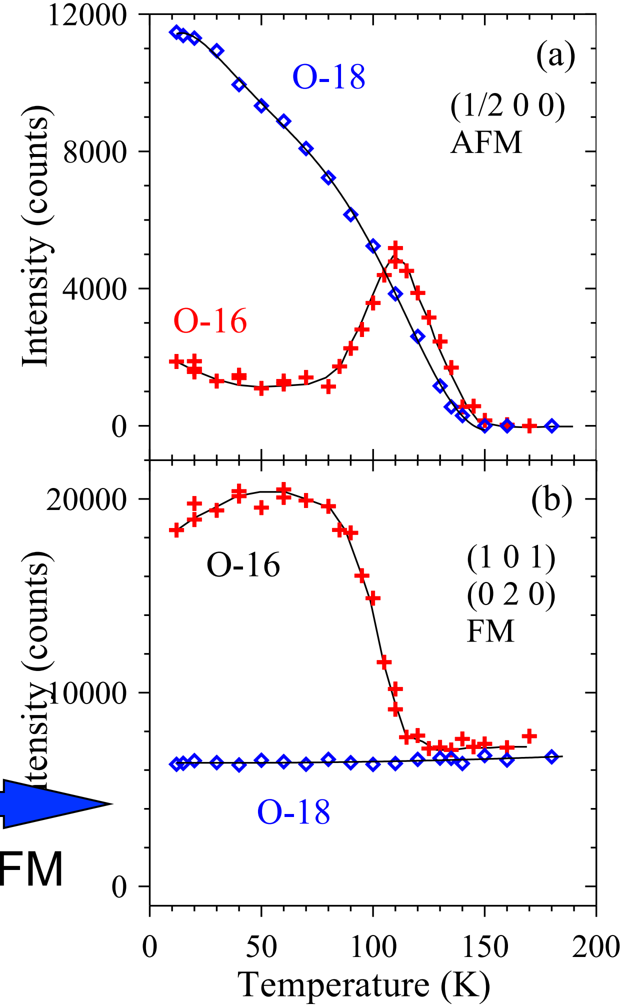

FM suppressed ⟷ No FM

Saturated effective magnetic moments in $(La_{1-y}Pr_y)_{0.7}Ca_{0.3}MnO_3$

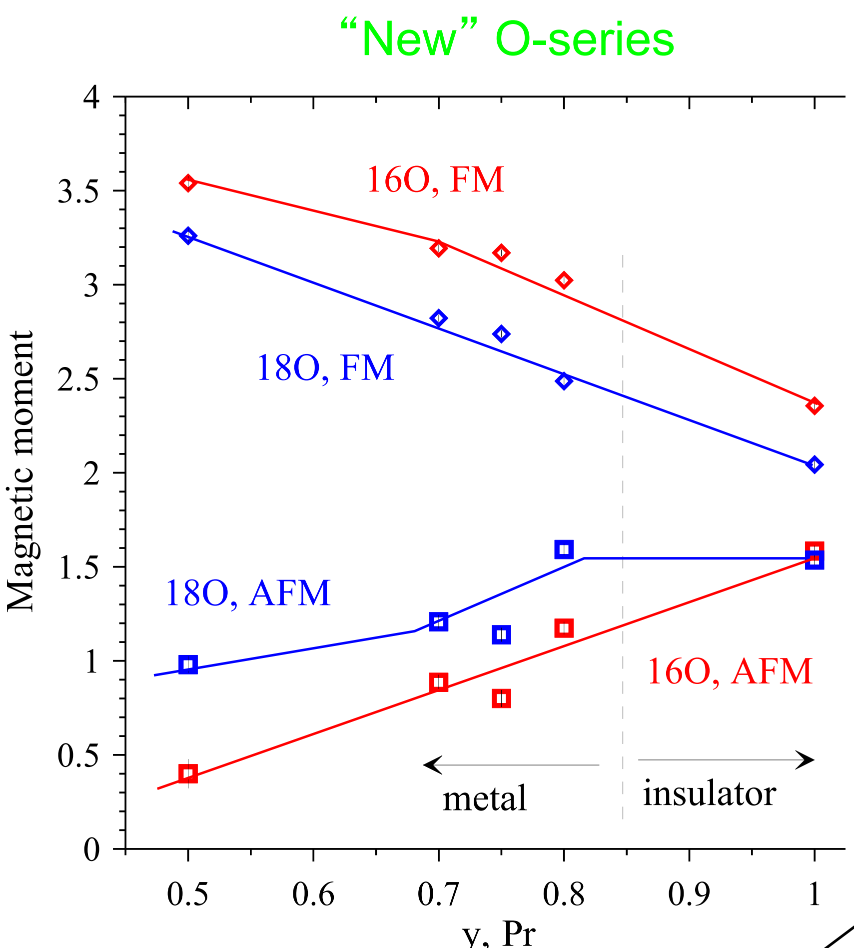

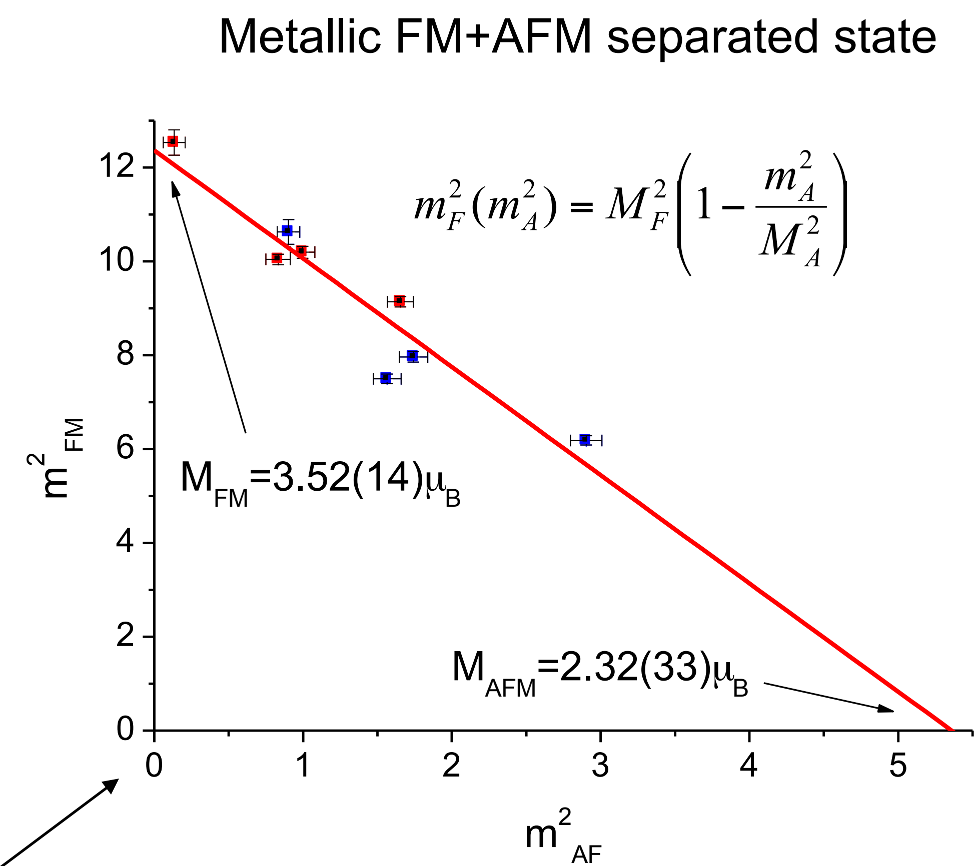

Effective moments

$m_{AF} = \nu^{1/2} M_{AF}$

$m_F = (1-\nu)^{1/2} M_F$

Volume fraction

Saturated effective magnetic moments in $(La_{1-y}Pr_y)_{0.7}Ca_{0.3}MnO_3$

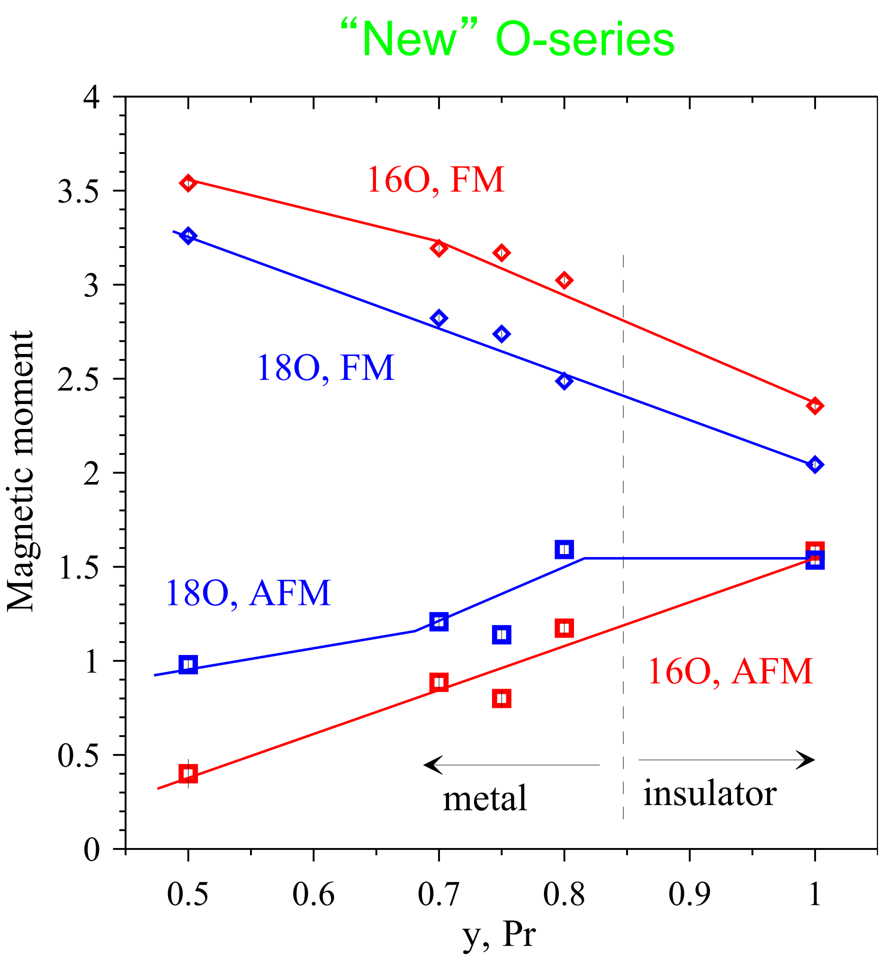

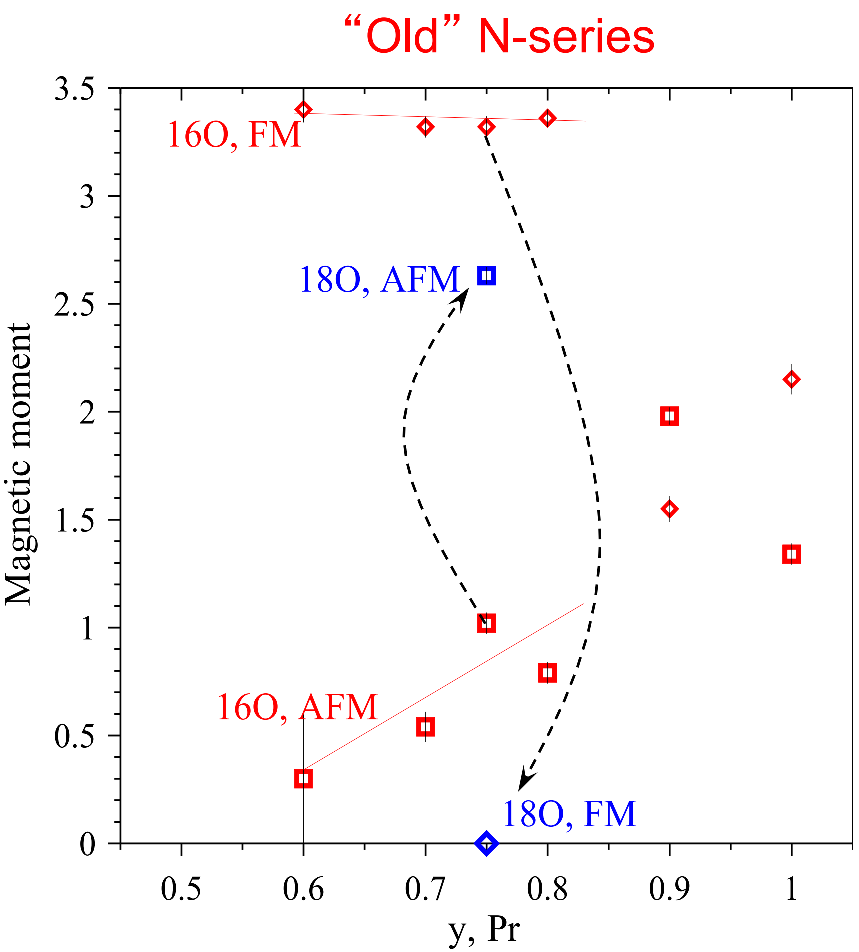

Effective moments

$$\begin{cases} m_{AF} = \nu^{1/2} M_{AF} \\ m_F = (1-\nu)^{1/2} M_F \end{cases}$$

Volume fraction

What is the difference between two series? Crystal structure?

$(La_{1-y}Pr_y)_{0.7}Ca_{0.3}MnO_3$, y=0.75 from both N- and O-series
Pnma, single phase at 290K

SLS X-ray material beamline.
Ultra-high resolution. λ=0.9A

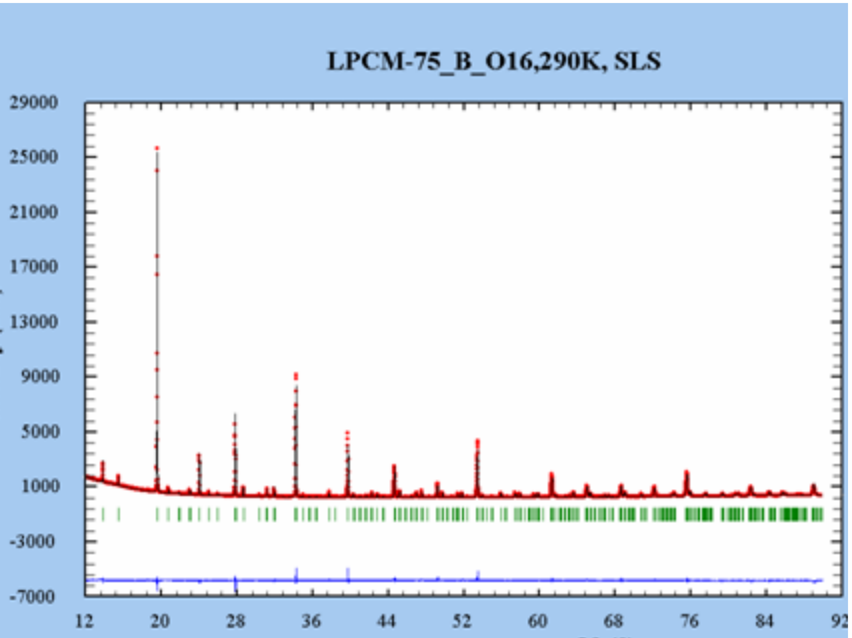

R_p=4%

HRPT/SINQ diffraction pattern.
λ=1.9A, HI-mode

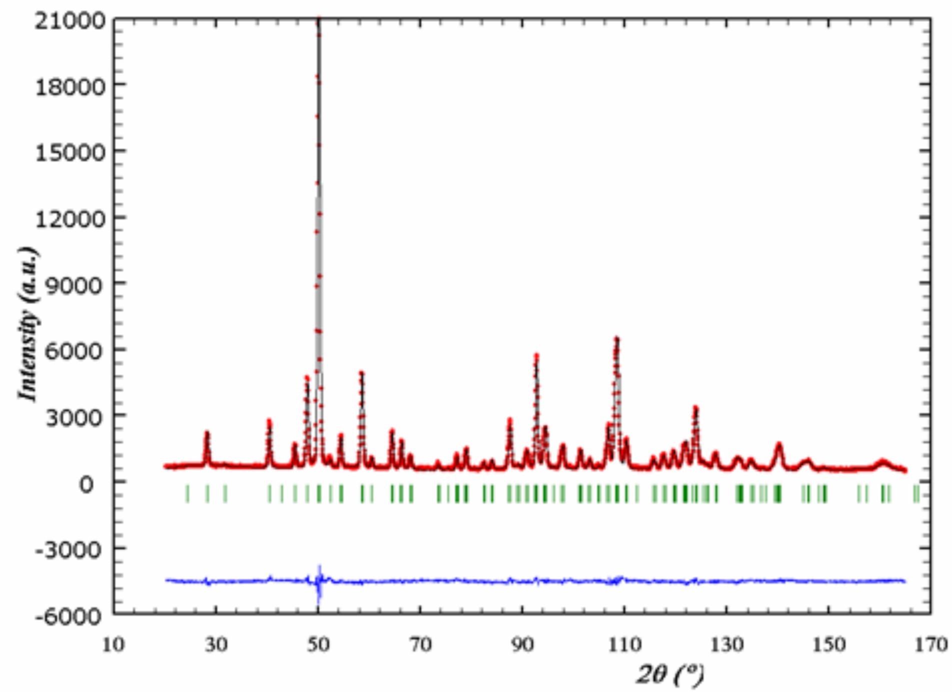

R_p=3.4%, χ^2=3

Comparison of lattice parameters

Pnma

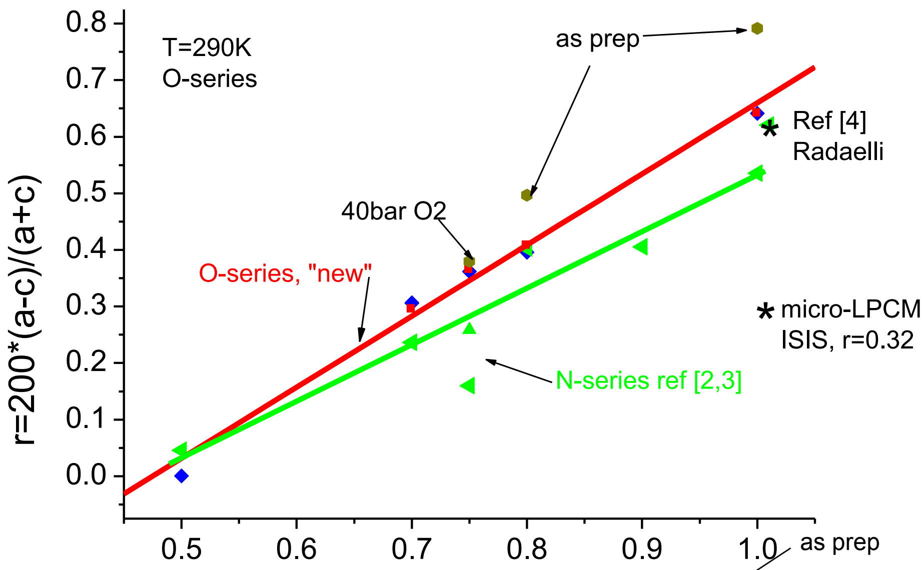

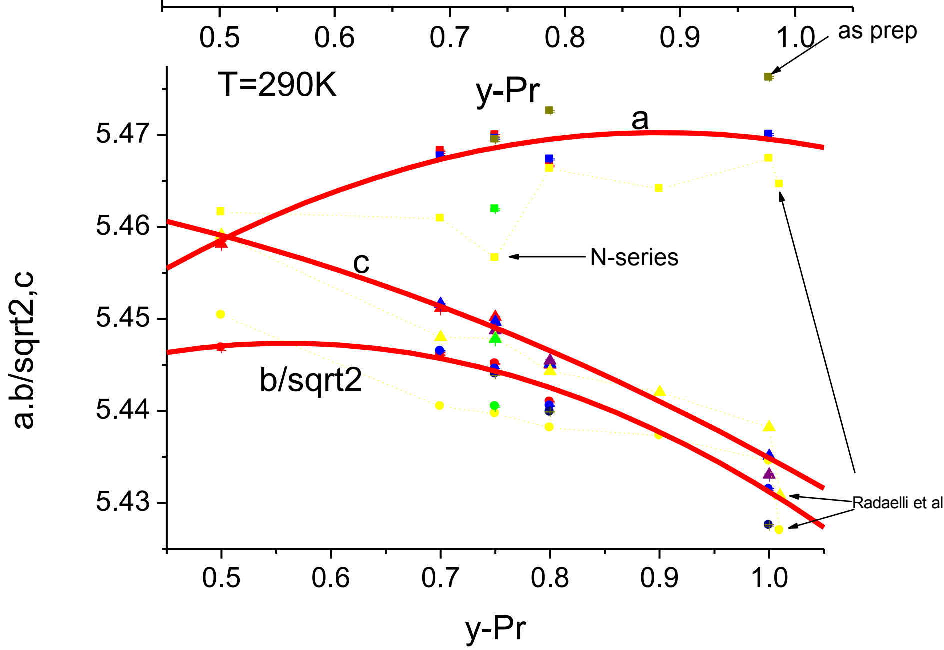

$(La_{1-y}Pr_y)_{0.7}Ca_{0.3}MnO_3$,

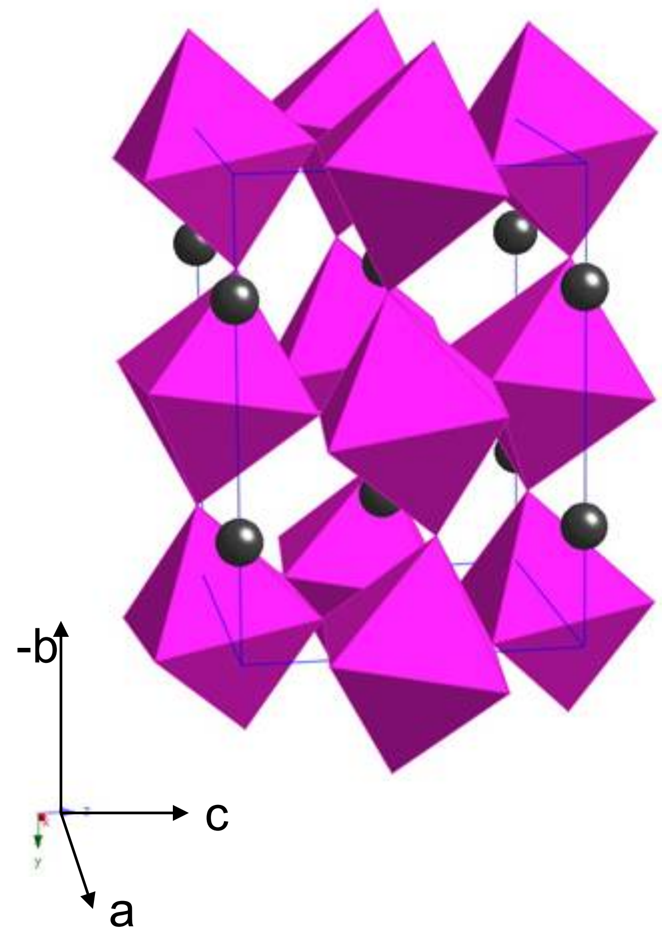

Bragg peak widths. Synchrotron X-ray, HRPT

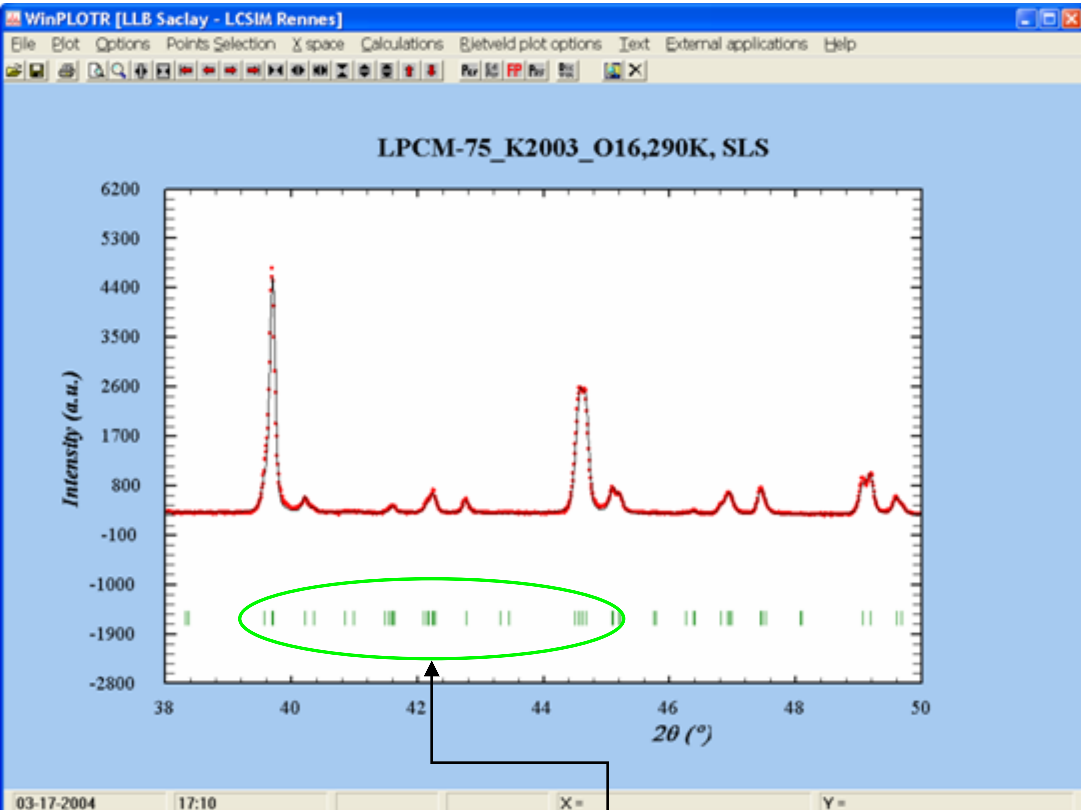

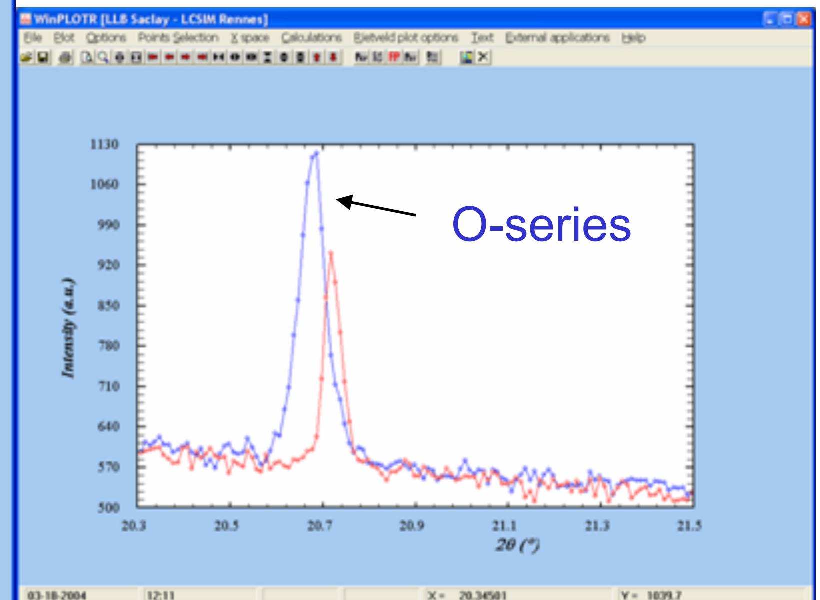

Pseudo-cubic metrics:
Strong peak overlap

Deconvolution of the Bragg-peak widths. Comparison of HRPT and synchrotron

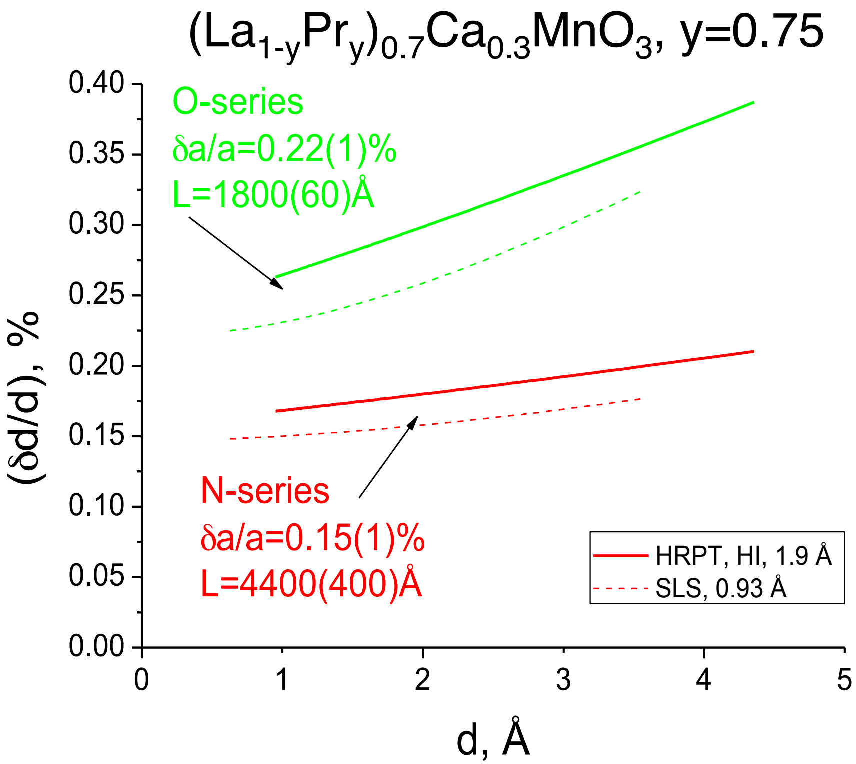

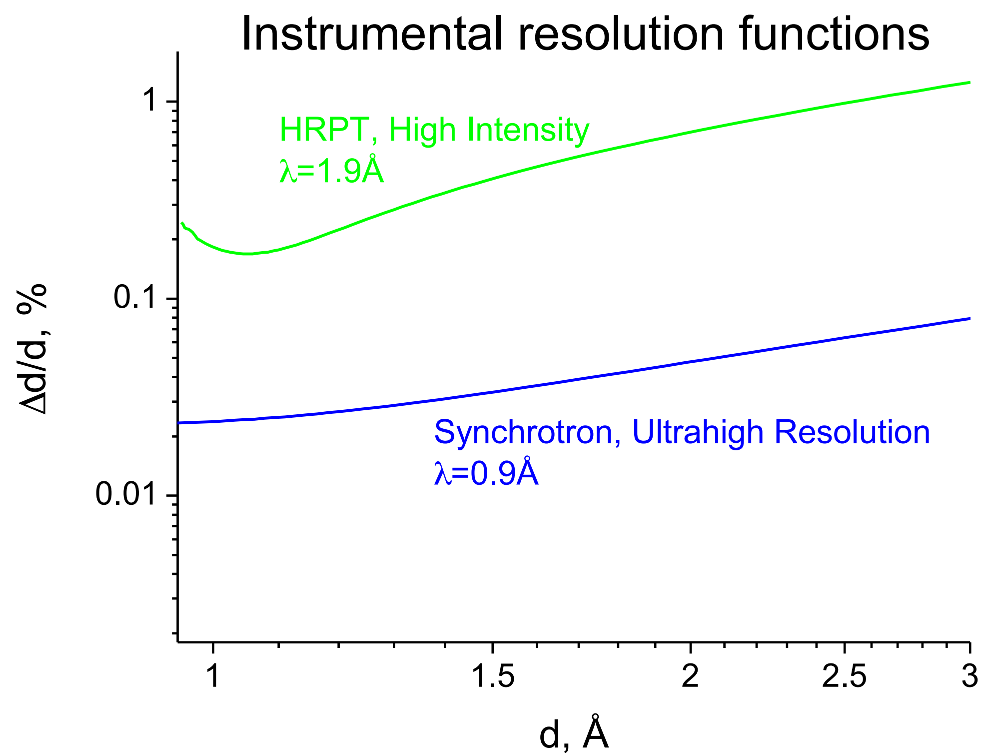

$$I_{exp}(2\theta) = \int_{-\infty}^{\infty} PV_{sample}(2\theta - \xi) PV_{instrument}(\xi) d\xi$$

Lorenzian ⊗ Gaussian

Thermal cycling through T_C

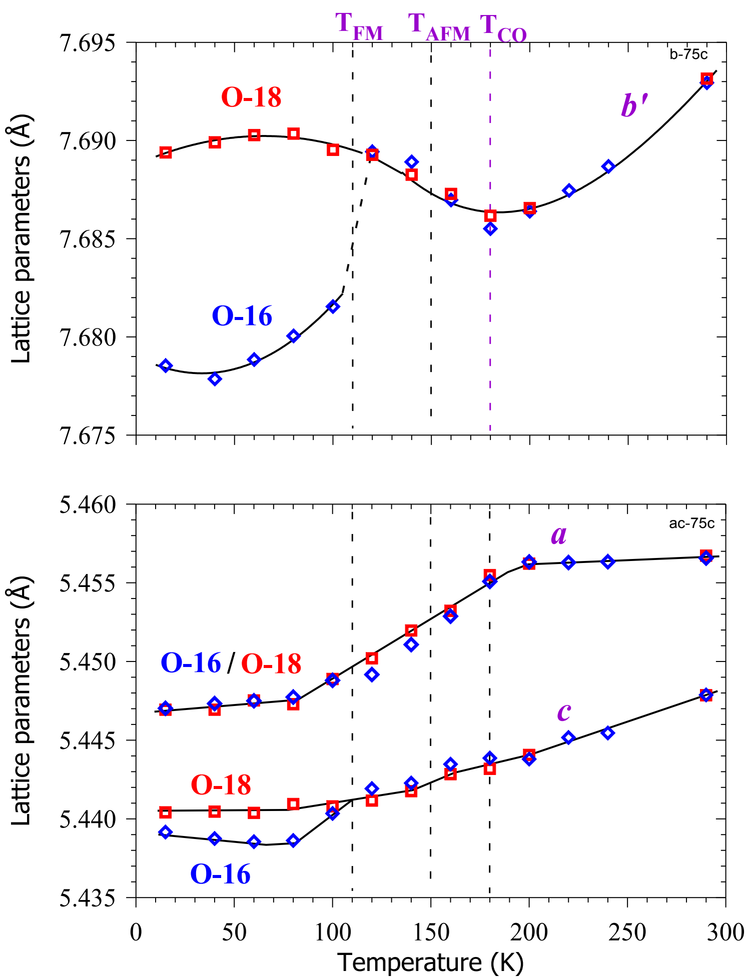

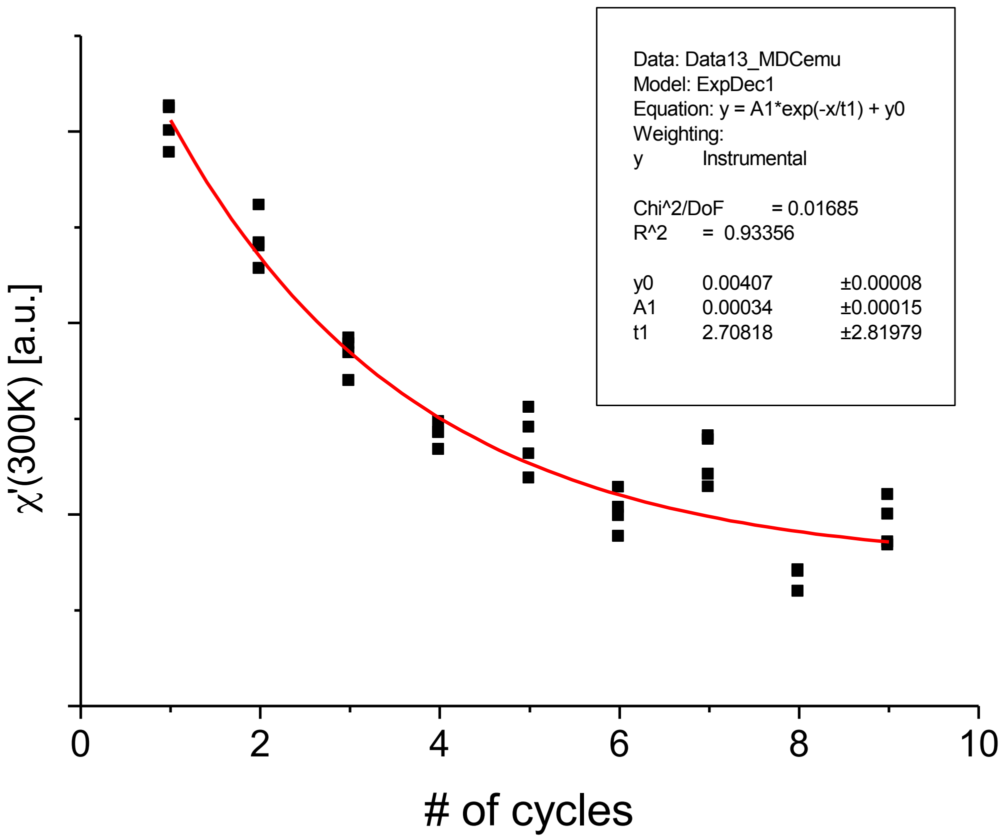

y=0.75

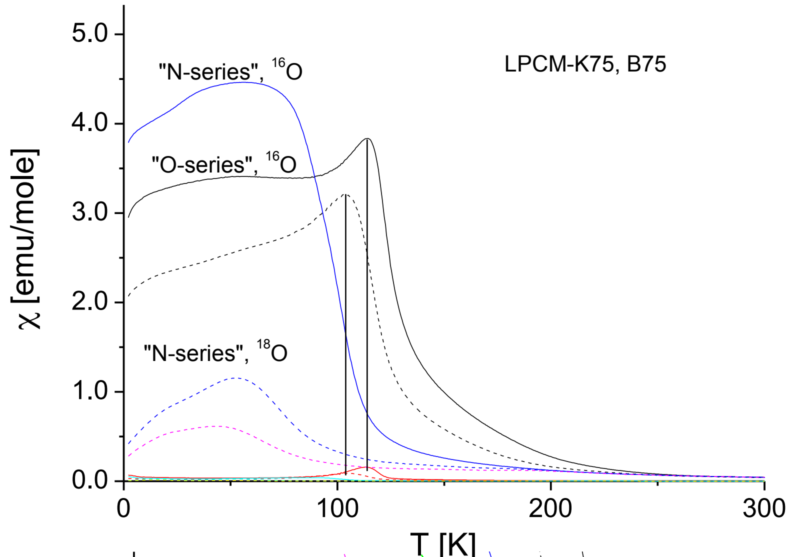

LPCM-K75, B75
"N-series", 16O
"O-series", 16O
"N-series", 18O
χ [emu/mole]
T [K]

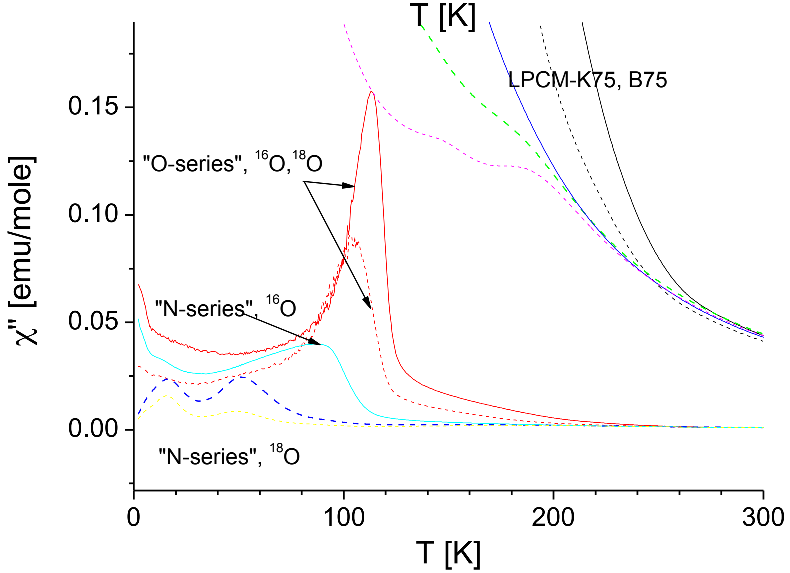

LPCM-K75, B75
"O-series", 16O,18O
"N-series", 16O
"N-series", 18O
χ" [emu/mole]
T [K]

DMC pattern

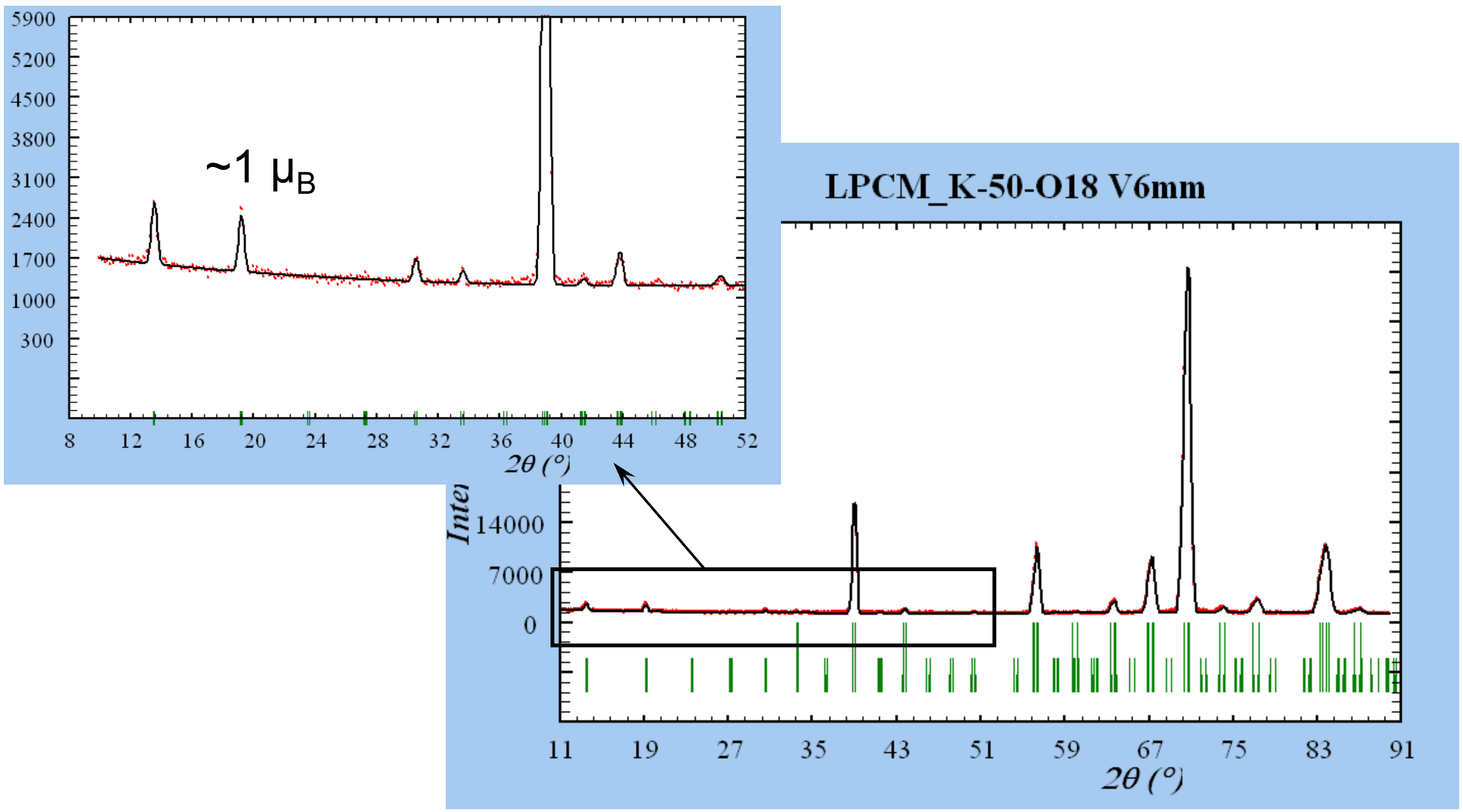

5900
5200
4500
3800
3100
2400
1700
1000
300
~1 μB
8
12
16
20
24
28
32
36
40
44
48
52
2θ (°)
LPCM_K-50-O18 V6mm
Inte
14000
7000
0
11
19
27
35
43
51
59
67
75
83
91
2θ (°)